Seismicity Patterns on Fault Zones with Different Geometrical and Rheological Properties

Yehuda Ben-Zion (USC) and many others

Patterns of earthquakes and faults are highly complex, having large apparent unpredictability associated at present with considerable **"ignorance"** and possibly also some inherent dynamic uncertainty.

Routes for progress:

•More and better data (seismicity, geodesy, lab experiments, precarious rocks, asymmetry of rock damage in fault zones, …….)

•Better analysis tools (ETAS, SSLIB, ZMAP, CSEP, CORSSA, improved location algorithms, improved focal mechanisms, ……)

•**Better physical understanding** providing "organizational principles" that can lead to higher resolution information with the available data and tools.

A theory for physics of earthquake does not exist! How can we have confidence that the theoretical results are relevant to nature?

Practical approach adopted here: Use multiple theoretical frameworks and search for emerging self-consistent results compatible with multi-disciplinary field and lab data.

Key Questions:

- How are geometrical, mechanical, and rheological properties of fault zones and their surrounding media related to different types of earthquake patterns in space-time-energy domains (e.g., localized vs. distributed spatial structures, power-law vs. characteristic frequency-size (FS) statistics, quasi-periodic vs. clustered temporal behavior, Omori-Utsu aftershock sequences vs. swarm response).

- Are there connections between different types of earthquake patterns considered usually in isolation (e.g., are the forms of FS and temporal statistics related, and if yes how)?

- When and how can we extrapolate results of low magnitude seismicity to large earthquake behavior?

- On what time scale is the seismic response to tectonic loading stationary, if at all?

We address these questions with continuum-mechanics & statistical-physics frameworks associated with three hierarchies of space-time scales:

(I) Long deformation history on a smooth homogeneous fault in elastic solid [e.g., Rice and Ben-Zion, 1996; Ben-Zion and Rice, 1997; Lapusta et al., 2000; Hillers et al., 2006, 2007].

(II) Seismicity on a discrete fault zone with fixed strong heterogeneities in elastic solid [e.g., Ben-Zion and Rice, 1993, 1995; Ben-Zion, 1996; Fisher et al., 1997; Dahmen et al., 1998; Zöller et al., 2004, 2005, 2007; Dahmen and Ben-Zion, 2007].

(III) Coupled evolution of earthquakes and faults in a regional lithospheric model with damage rheology [e.g., Lyakhovsky et al., 1997, 2001; Ben-Zion et al., 1999; Ben-Zion and Lyakhovsky, 2002, 2006; Finzi et al., 2007].

Main Results

There are 3 general dynamic regimes:

- The first is associated with relatively smooth faults, FS statistics compatible with the characteristic earthquake distribution, quasi-periodic temporal occurrence of large events, and no accelerated seismic release before large events.

- The second is associated with disordered fault structures, power law FS statistics of earthquakes, temporal clustering of intermediate and large events, and accelerated seismic release before large earthquakes.

- For a range of conditions, there is a third regime in which the response switches back and forth between the forgoing two modes of behavior over multiple large earthquake cycles.

- In the latter cases, the seismic response of the fault zone is non-stationary on time scales shorter than several mode-switching intervals (e.g., 1000-10000 yr. for large fault zones).

- Cold regions have classical Omori-Utsu aftershock sequences with power law frequency-size statistics, while warm/hot regions have diffuse sequences or swarms without power law frequency-size statistics.

(I) A smooth homogeneous fault in elastic solid

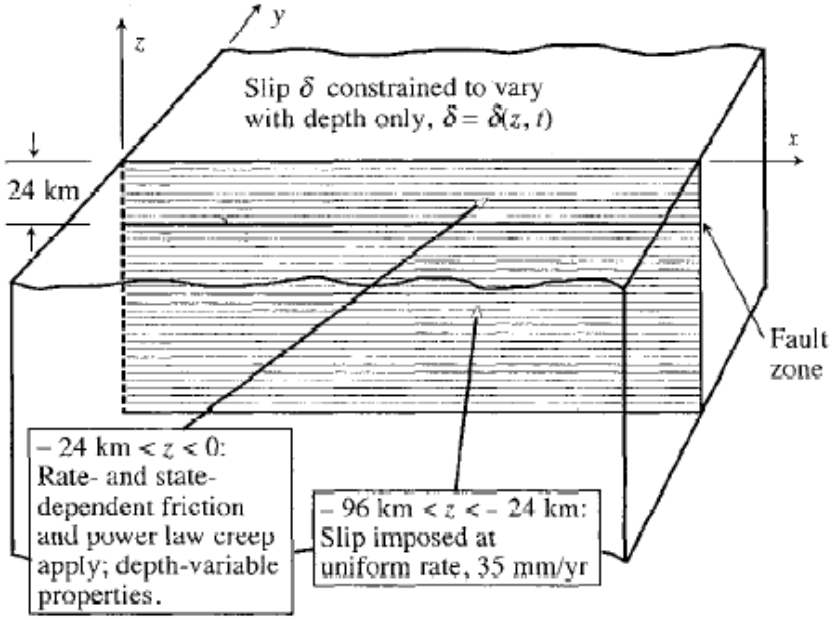

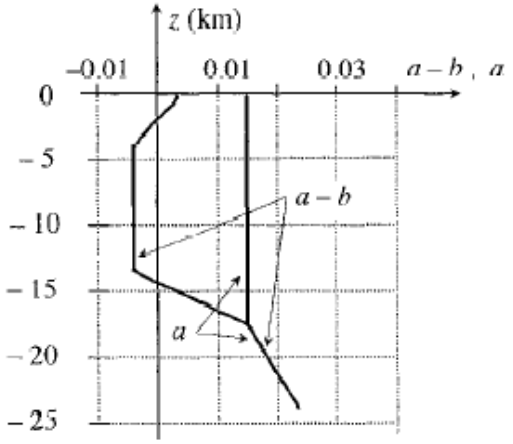

Rice and Ben-Zion, 1996; Ben-Zion and Rice, 1997; Lapusta et al., 2000; Hillers et al., 2006, 2007.

Nucleation size for Brittle instabilities:
$h^* = 2\mu L/[\pi\sigma(b\text{-}a)]$

h* << *h* **is required to simulate a *smooth fault in an elastic continuum***

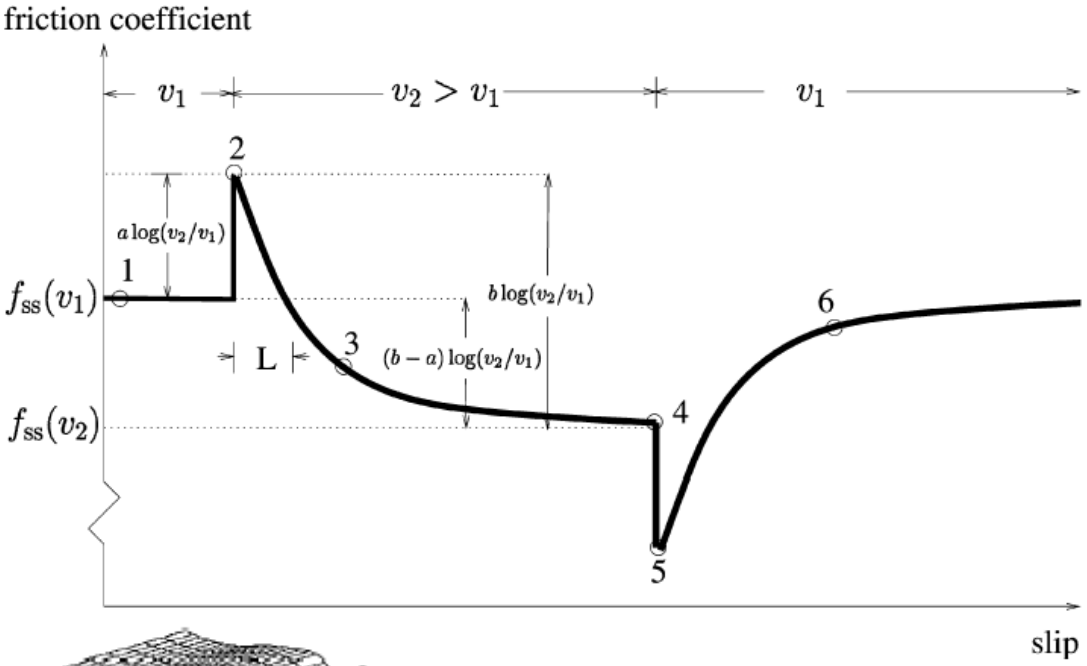

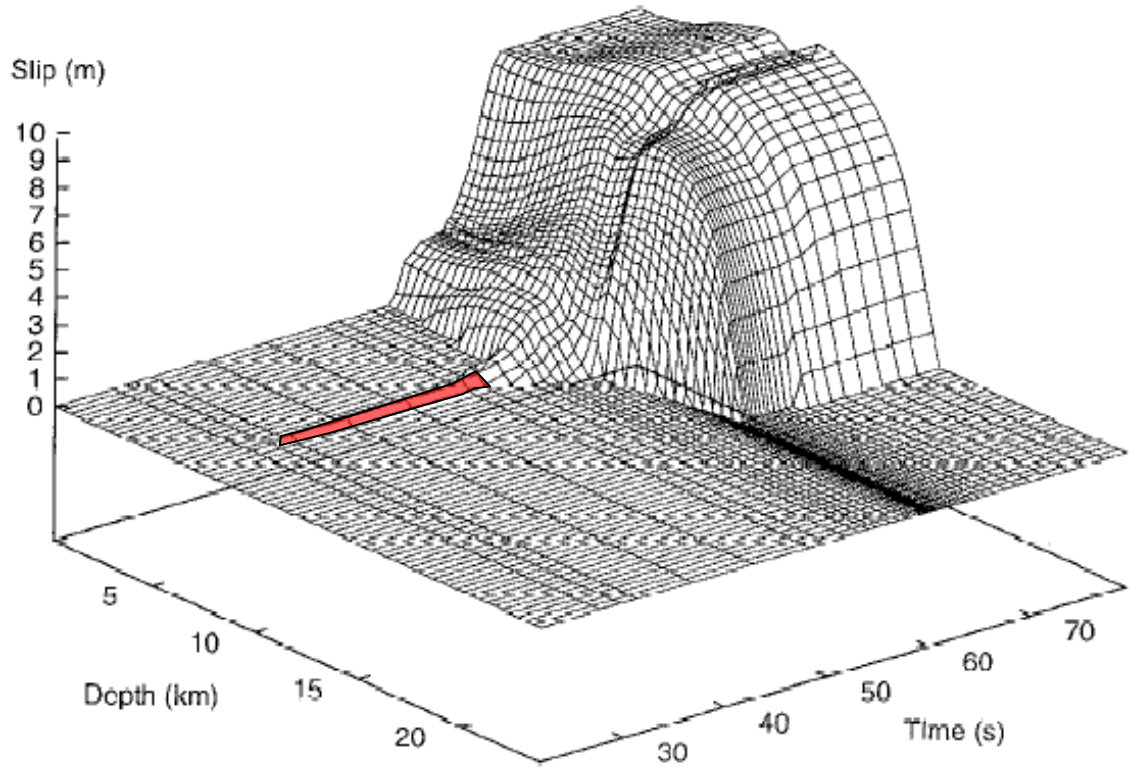

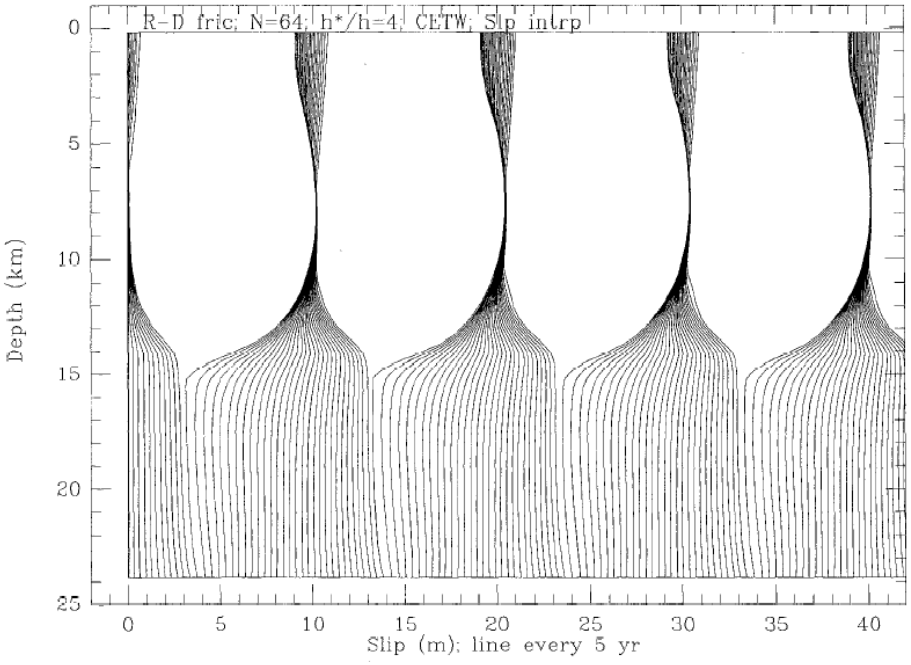

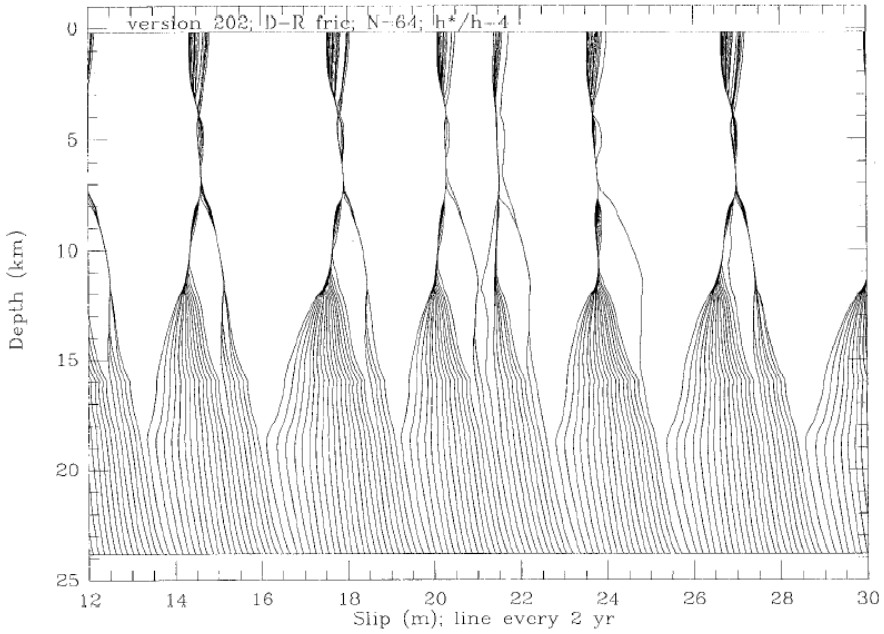

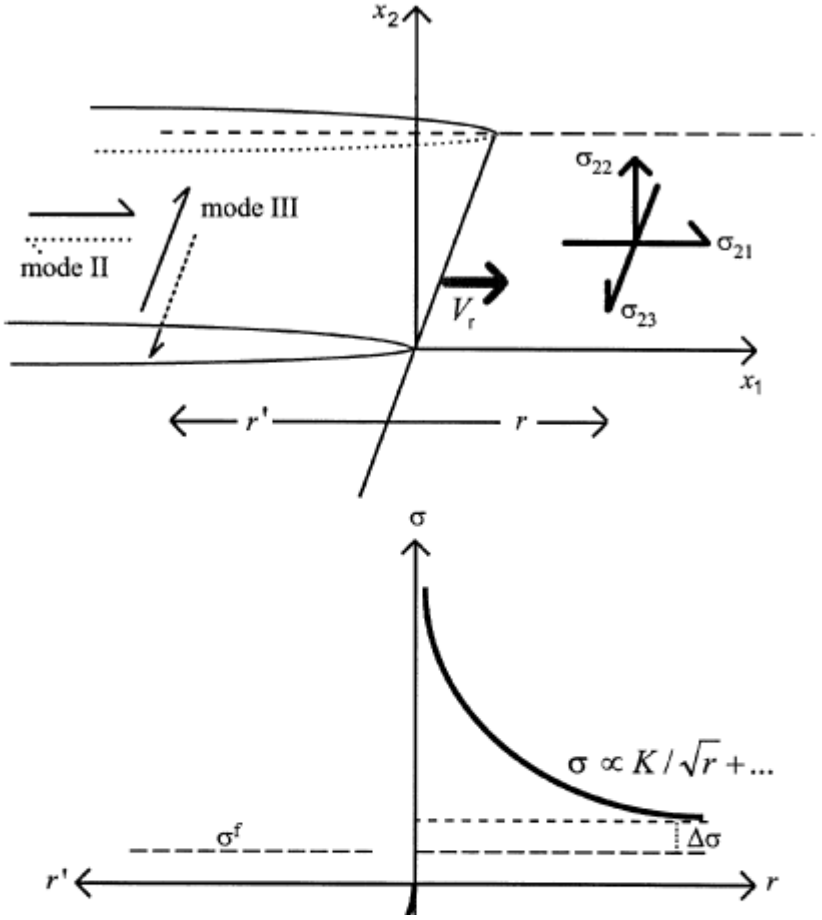

The large stress concentrations at the tip of propagating ruptures in a continuum tend to produce (quasi-periodic) system-size events.

Need strong heterogeneities to stop ruptures!

Hillers et al. (06, 07): rate-state with heterogeneous distribution of *L*

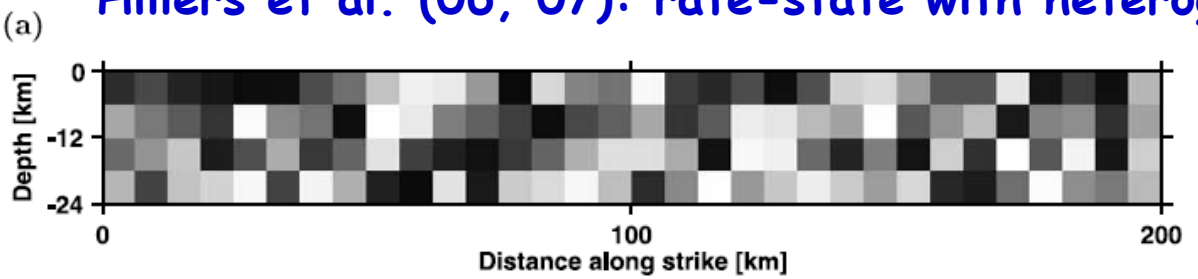

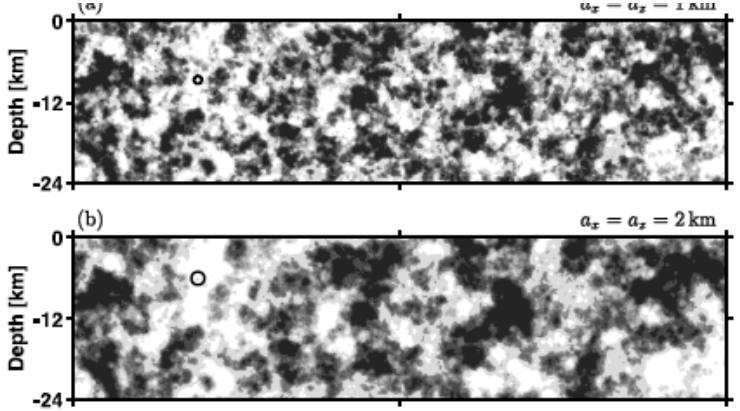

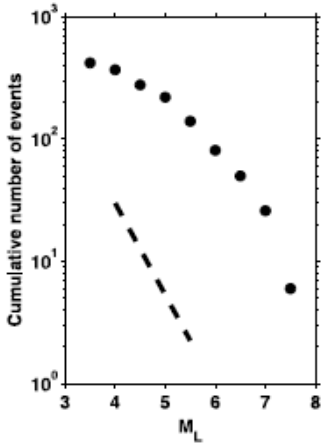

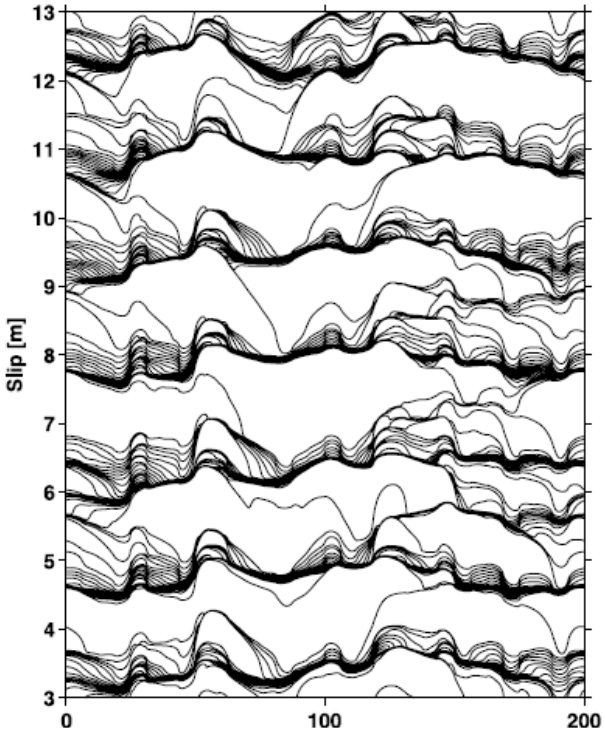

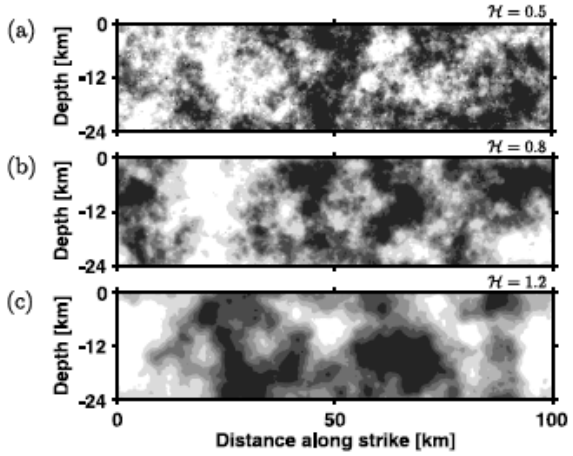

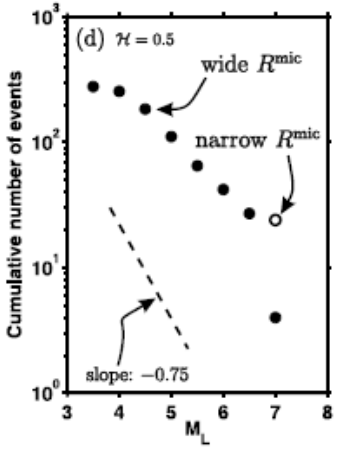

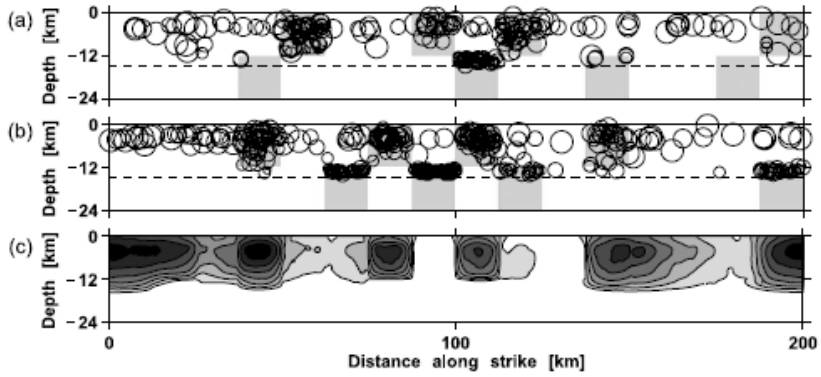

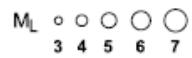

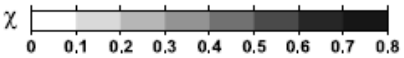

Main conclusion: increasingly realistic behavior for heterogeneities spanning wide range of size scales (e.g., large S.D.)

(II) Seismicity in (discrete) fault zones with fixed strong heterogeneities

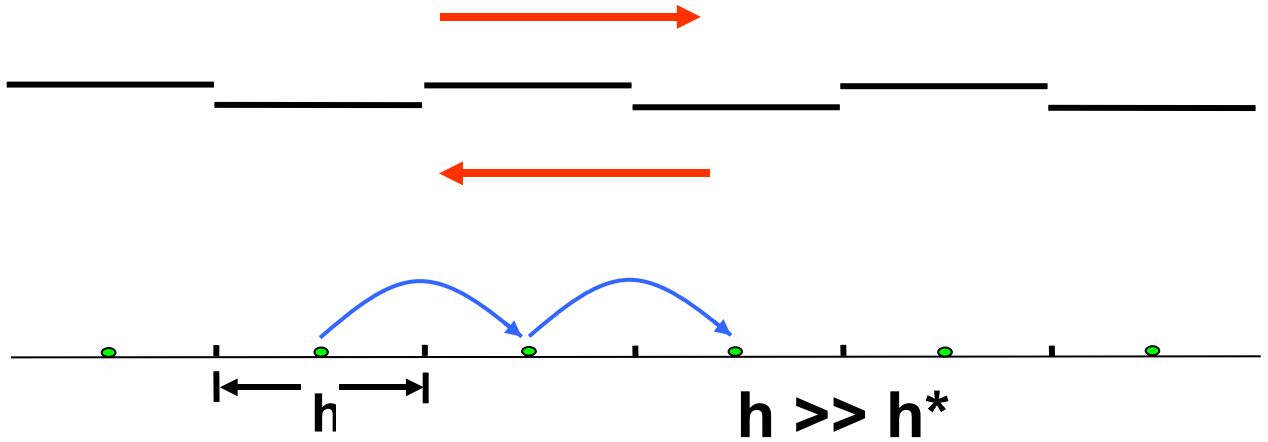

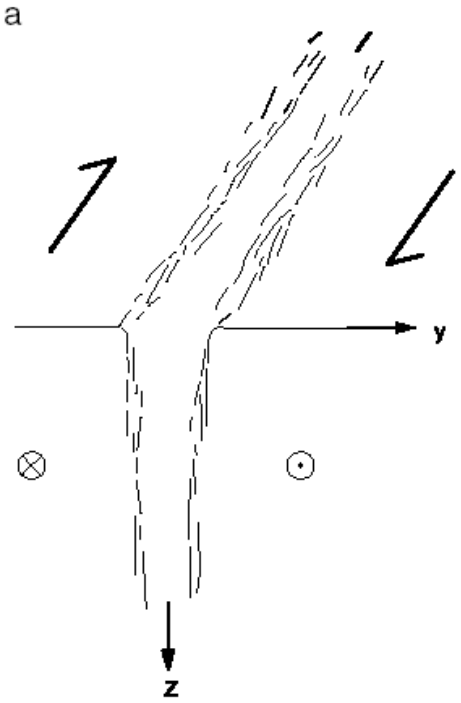

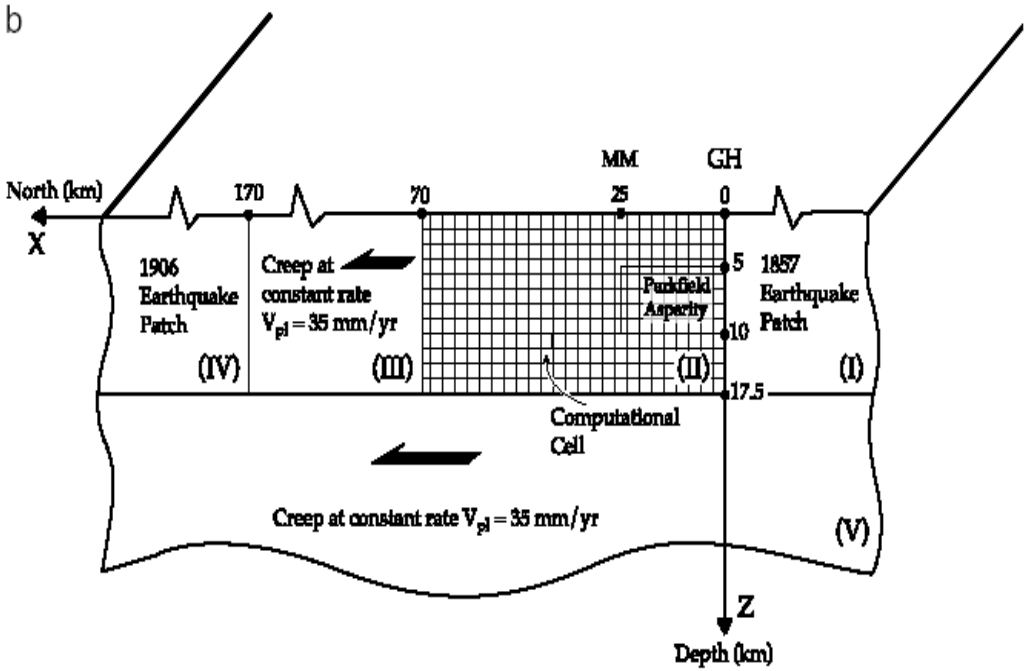

Ben-Zion and Rice, 1993, 1995; Ben-Zion, 1996; Fisher et al., 1997; Dahmen et al., 1998; Mehta et al., 2006; Zöller et al., 2004, 2005, 2007)

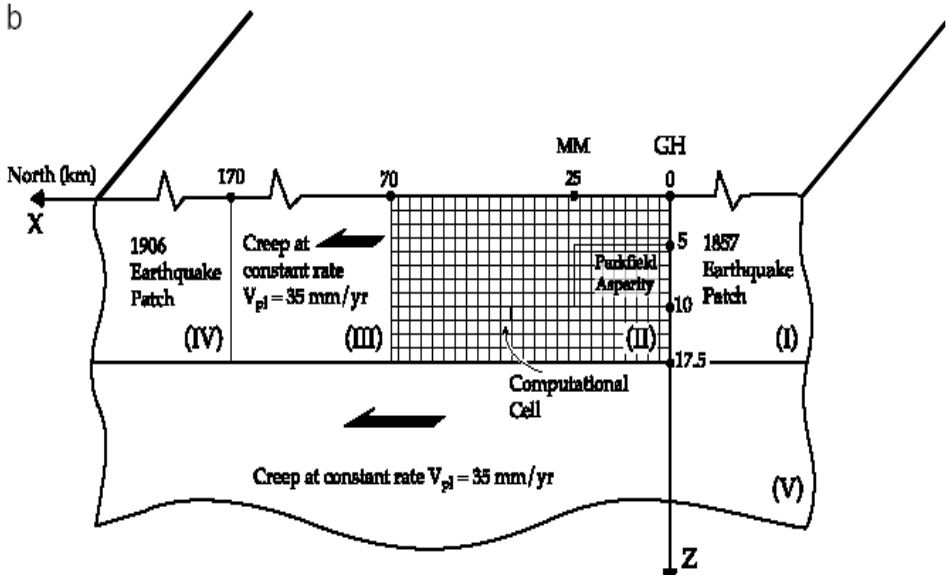

Focus:

-Heterogeneities spanning different ranges of size scale

-Different values of ϵ

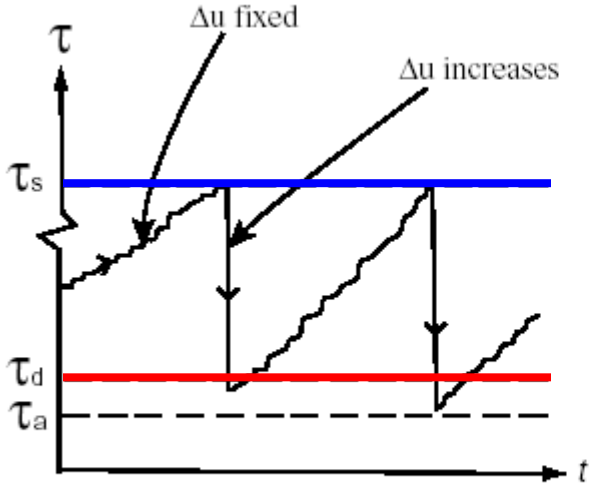

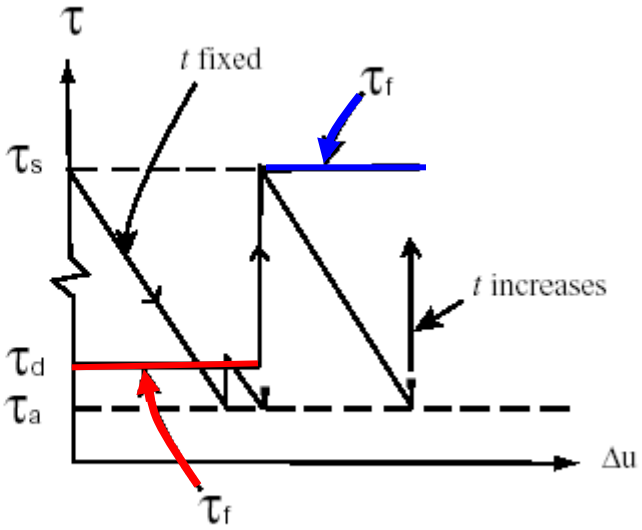

$\tau_d - \tau_a \equiv$ dynamic overshoot

$\epsilon = (\tau_s - \tau_d)/\tau_s =$ dynamic weakening

Frequency-size statistics for fault zones with Narrow Range of Size Scales ($\epsilon > 0$; $\tau_d < \tau_s$)

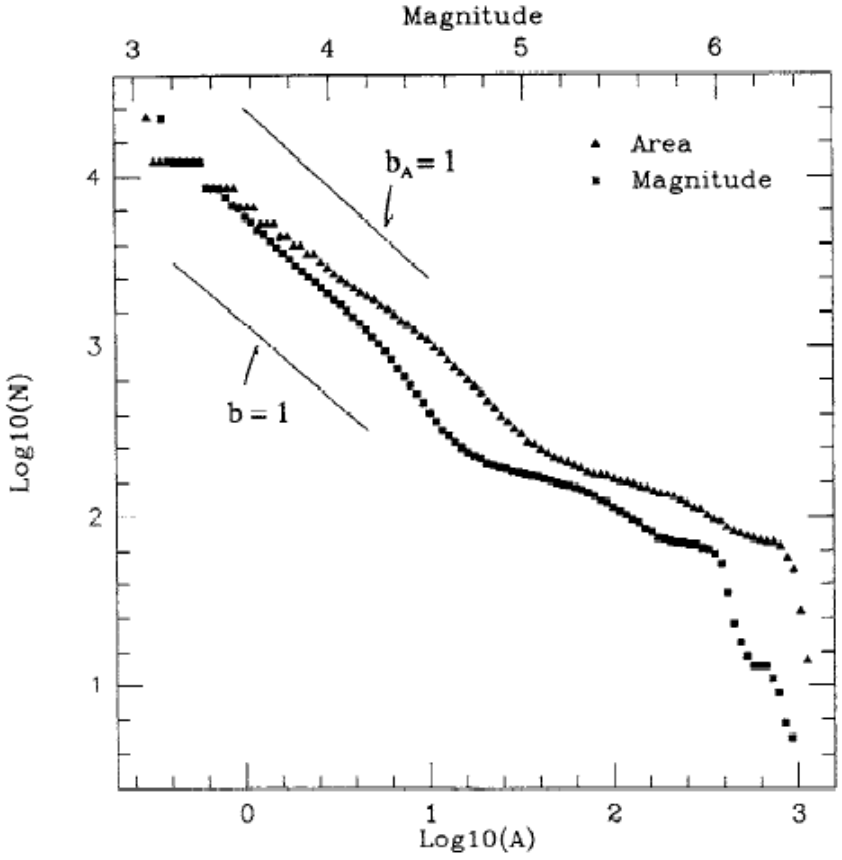

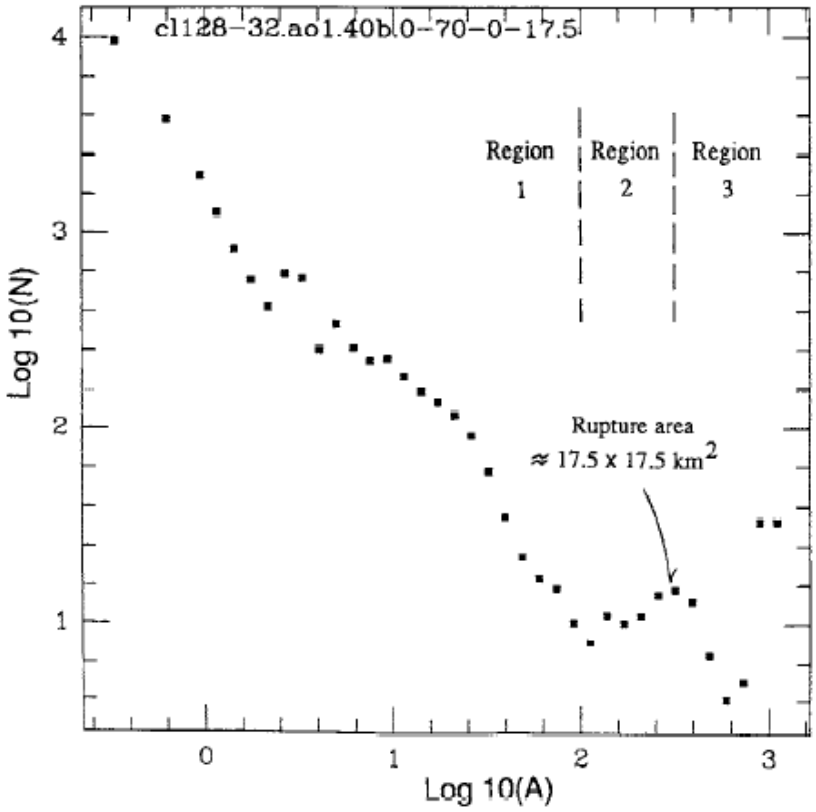

The breaking of self-similarity in the frequency-size statistics on relatively regular faults is produced by the scaling of stress concentration in elastic solid with rupture dimension.

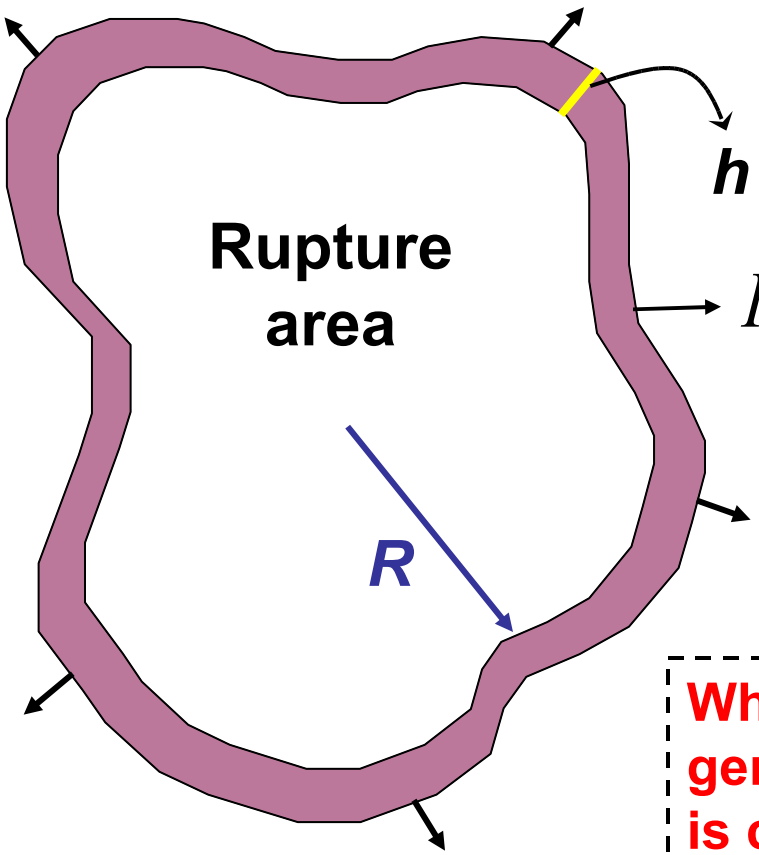

$$K \propto \sqrt{R} \quad , \tau = \tau_0 + \text{const}$$

Here $R^*_{crit} \tilde{K} 8h$

For homogeneous continuum fault, $R_{crit} \sim h^*$

When the rupture reaches a critical size, generating stress transfer to the edge that is comparable to the average stress drop, it becomes (statistically) a "runaway" event terminating the power law regime of earthquake statistics [Ben-Zion and Rice, JGR, 93')

Frequency-size statistics for fault zones with Wide Range of Size Scales ($\epsilon > 0$)

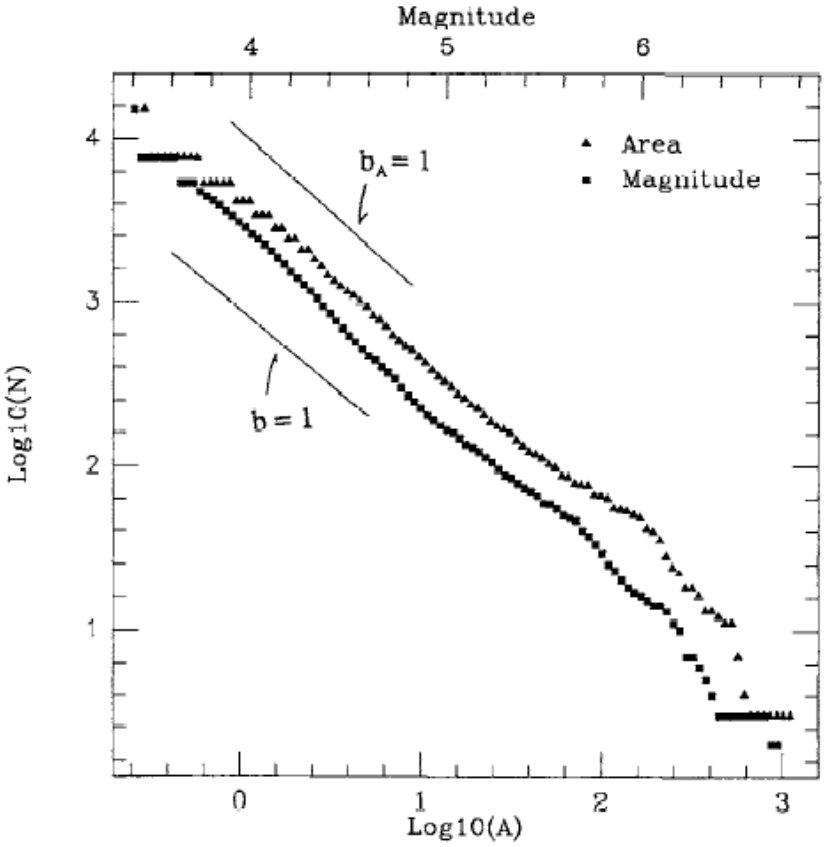

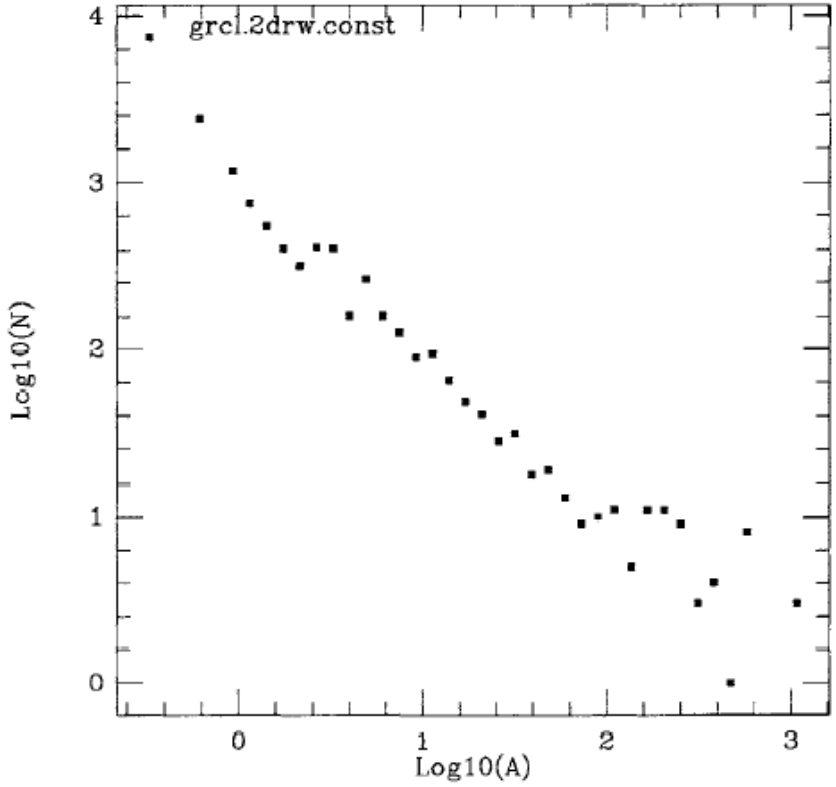

Relations to observations?

Wesnousky 1994

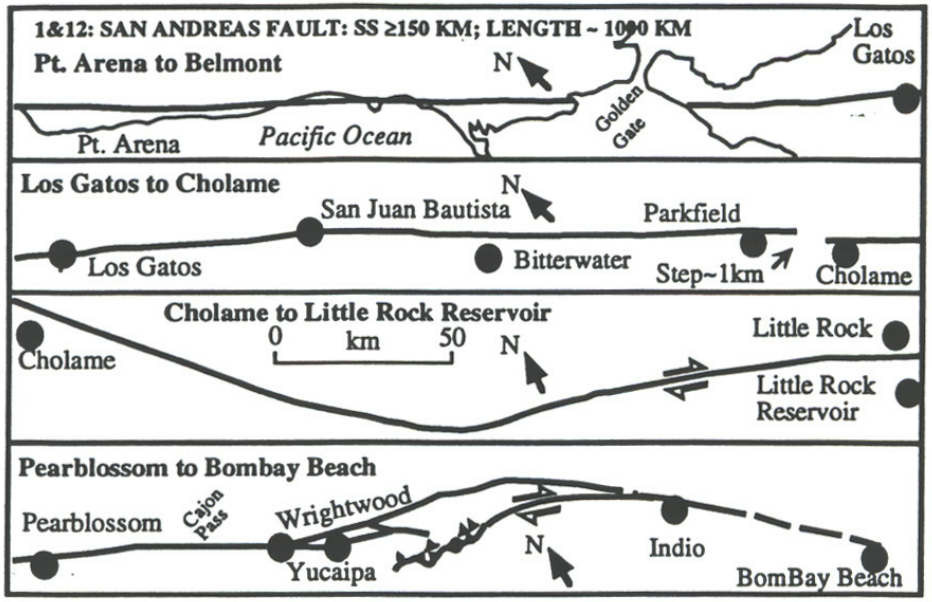

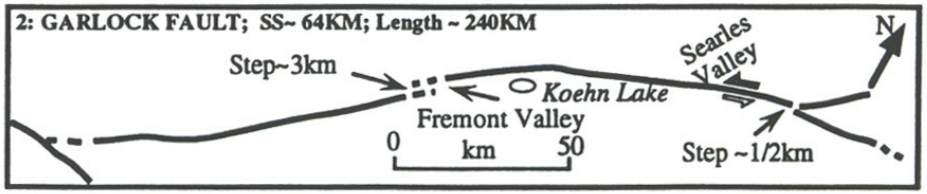

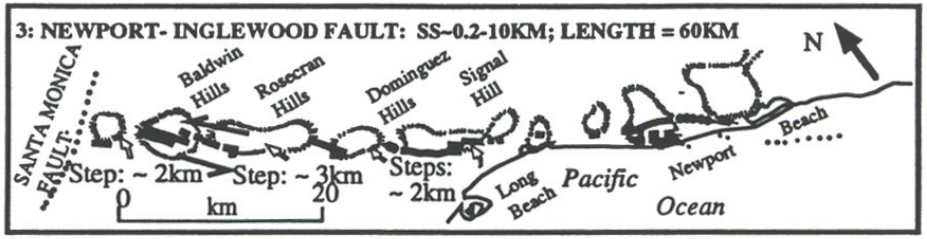

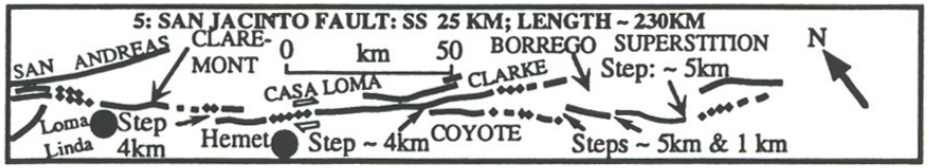

Relatively regular

Highly irregular

NROSS

WROSS

Statistics for highly irregular structure with WROSS are compatible with the Gutenberg-Richter distribution

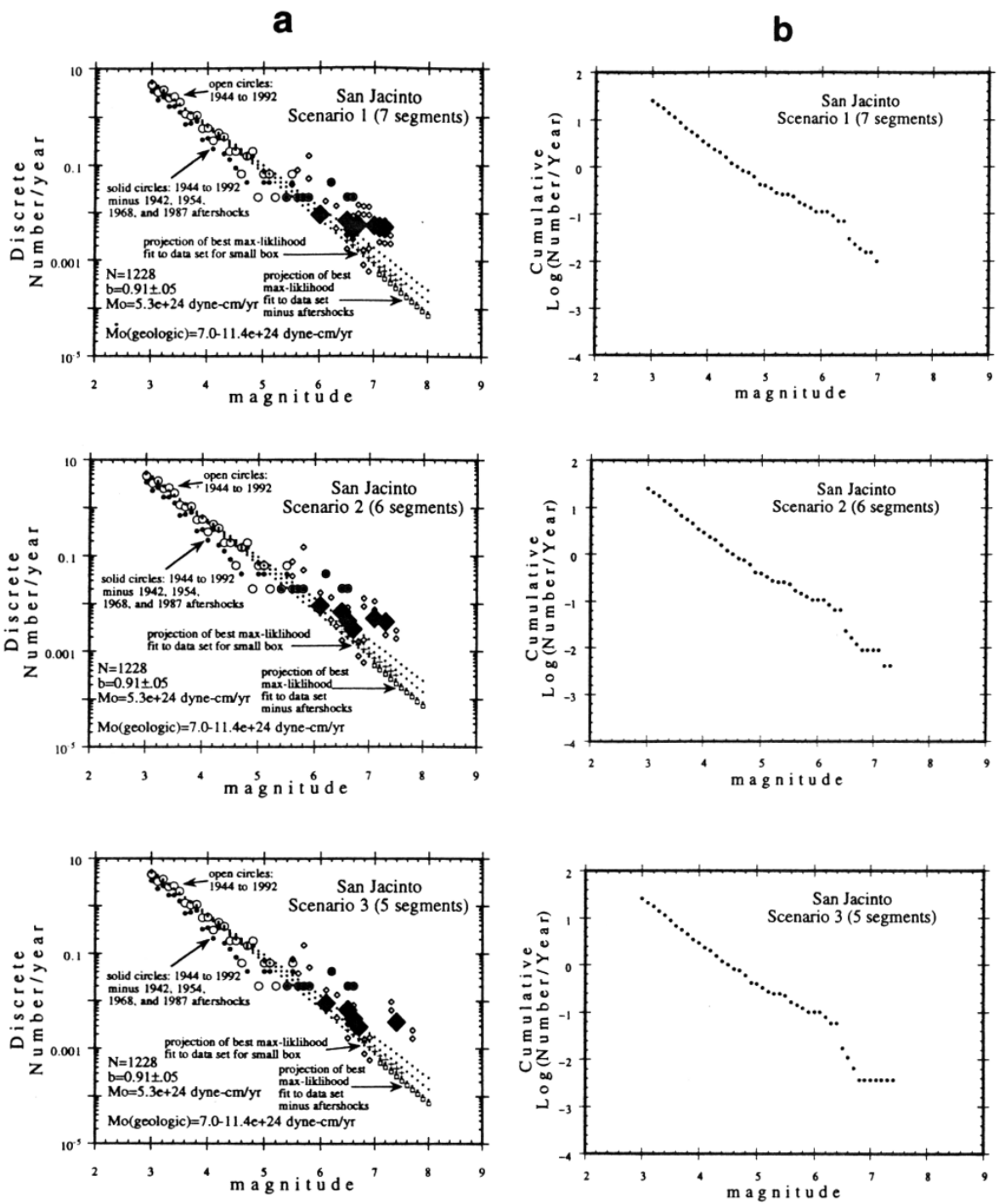

Statistics for relatively regular structure with NROSS are compatible with the Characteristic earthquake distribution

a

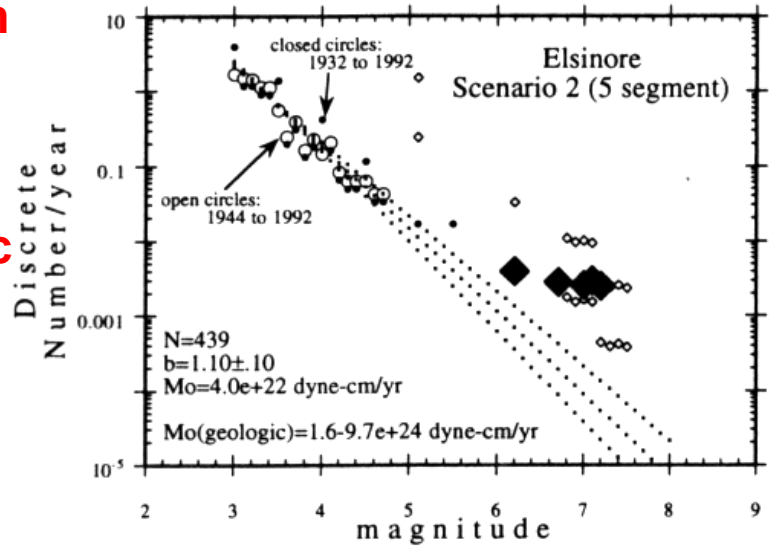

b

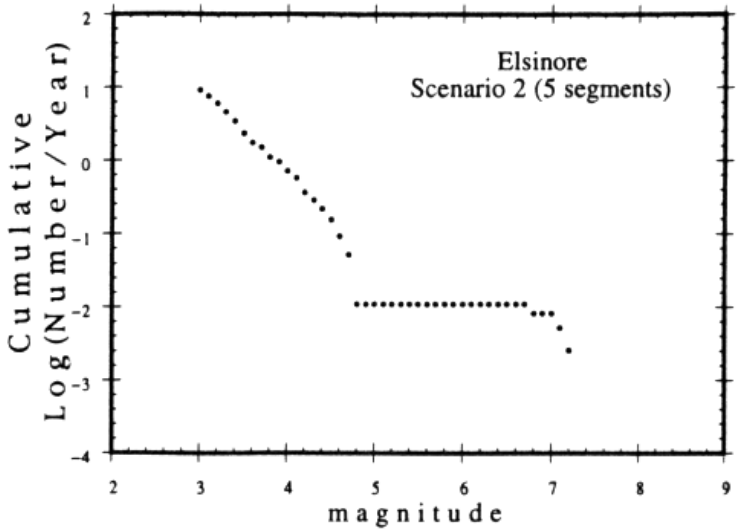

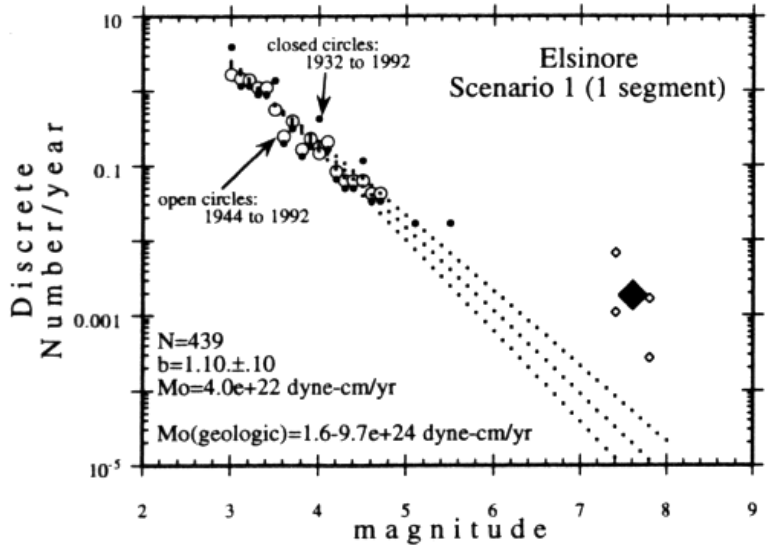

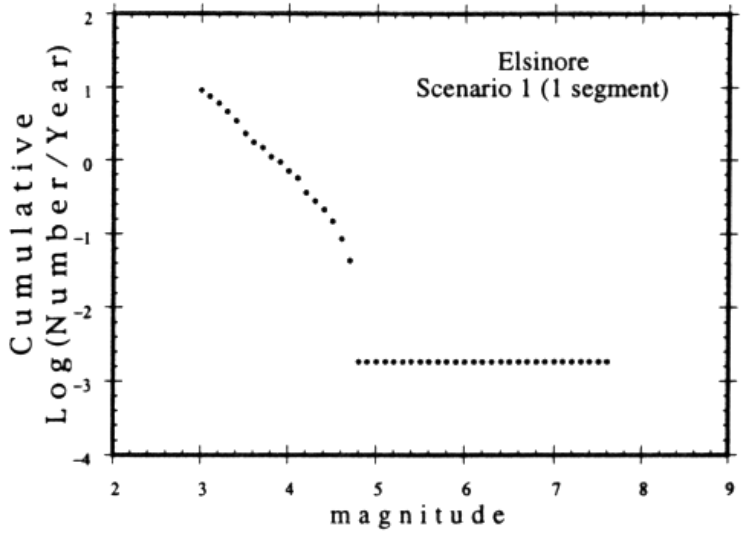

Statistics for relatively regular structure with NROSS are compatible with the Characteristic Earthquake distribution

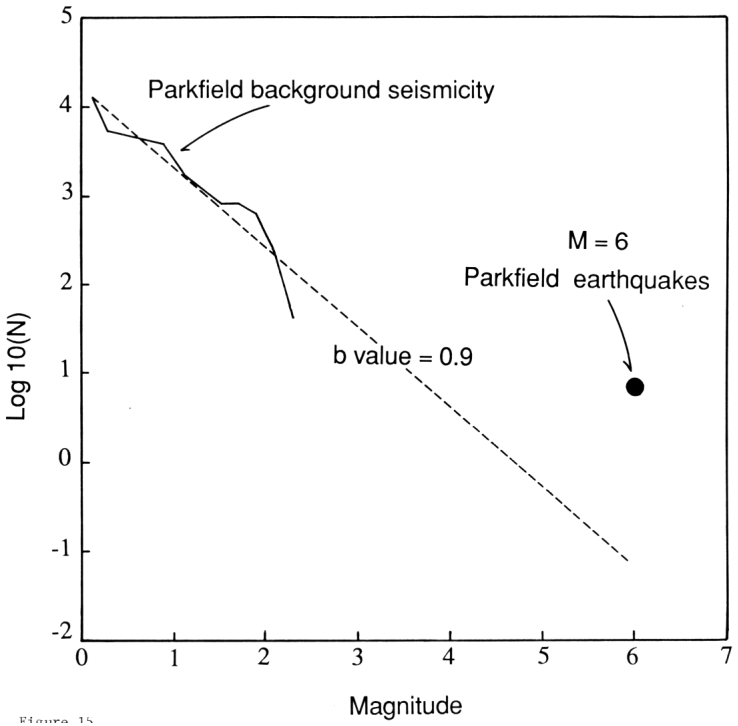

Discrete statistics for seismicity along the Parkfield section of the SAF (Ben-Zion and Rice, 1993)

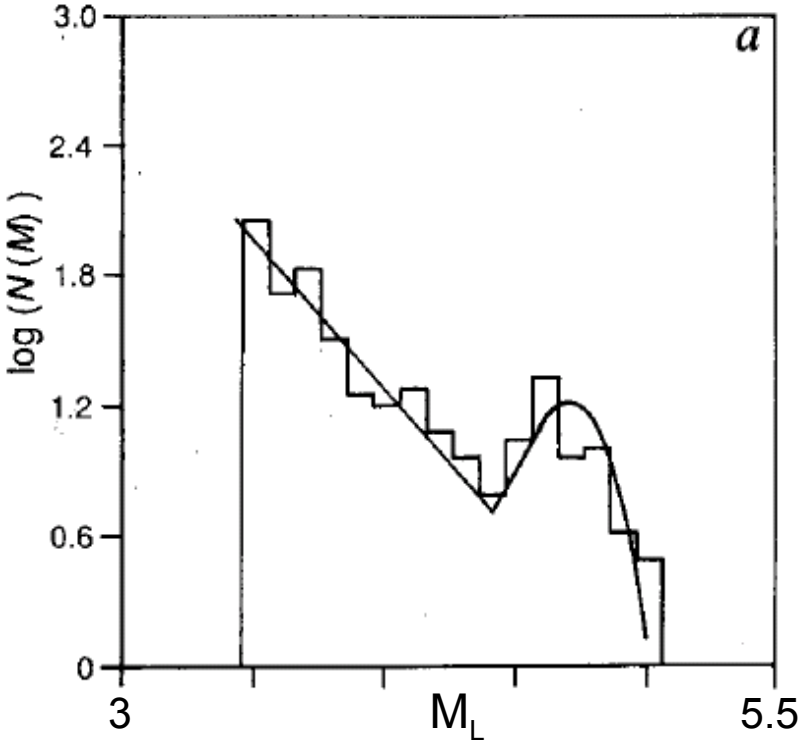

Discrete statistics for seismicity preceding the 1980 eruption of Mount St Helens (Main, 1992)

Temporal Statistics

Narrow ROSS

Wide ROSS

Small events (M>4.5)

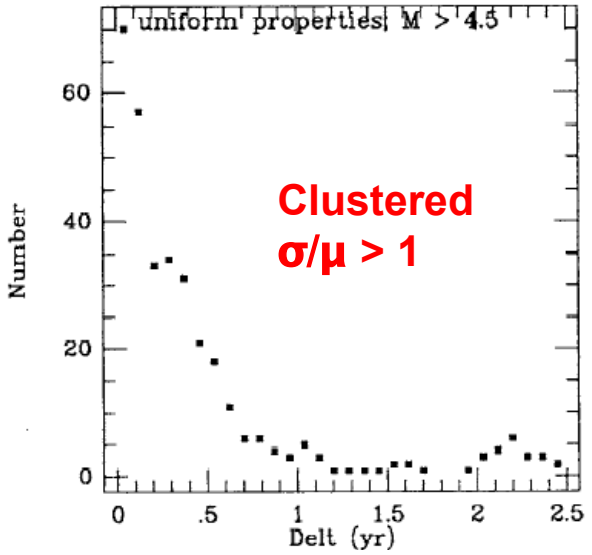

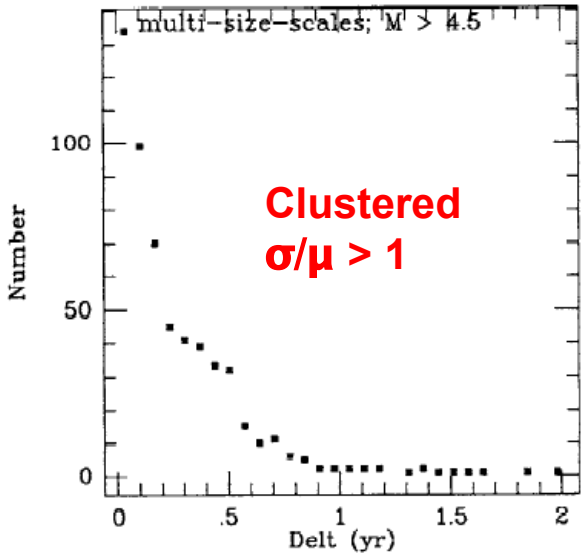

Large events (M>6)

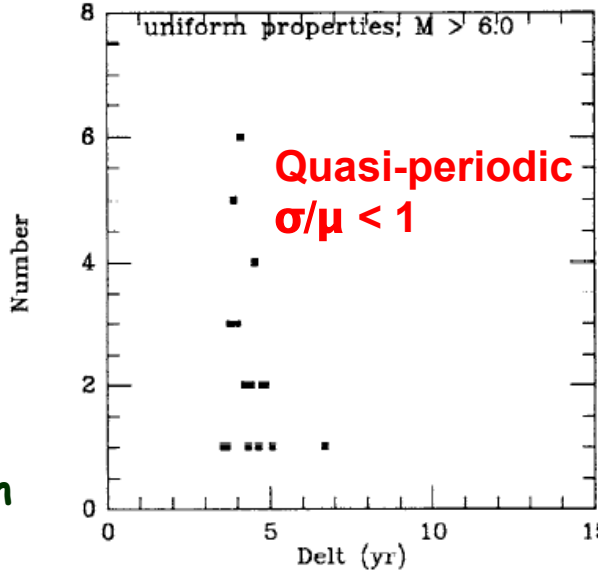

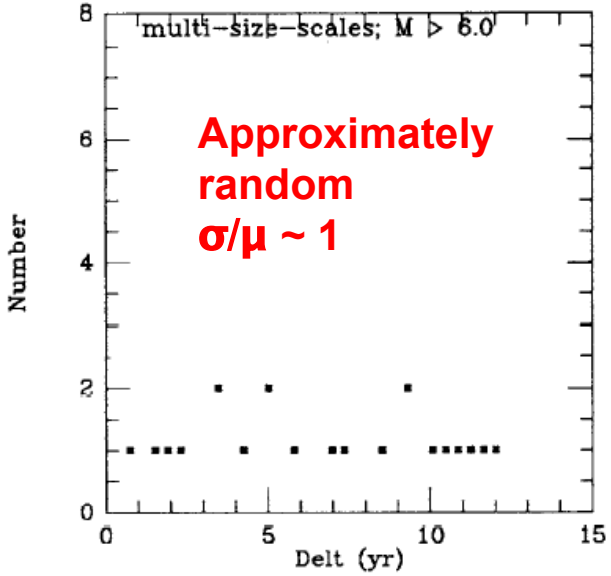

Zöller et al. (2004, 05, 06, 07) provide extensive additional related results.

See also Monday poster on recurrence intervals and hazard

A phase diagram of seismicity on faults with different levels of heterogeneities

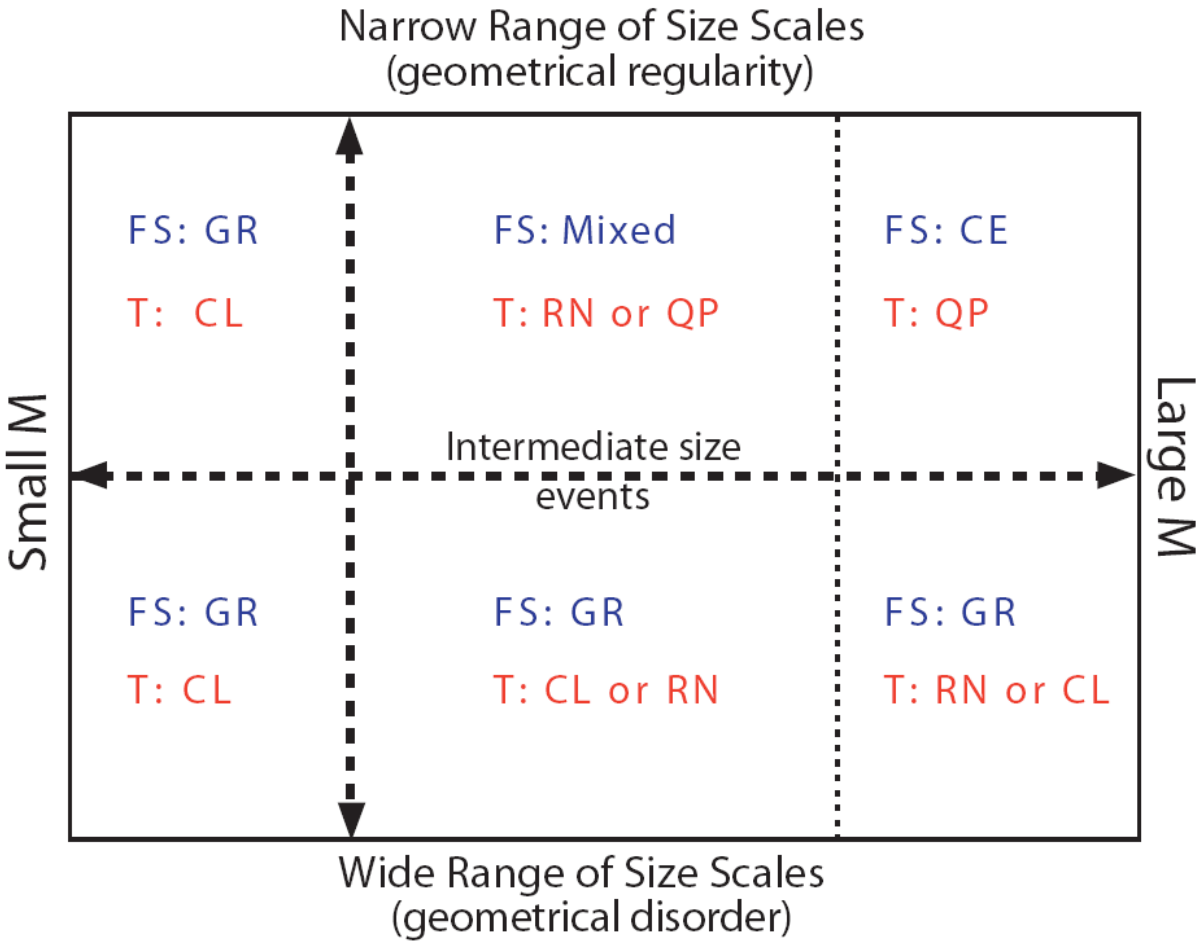

Frequency-size (FS) statistics: Gutenberg-Richter (GR) and Characteristic (CE)
Temporal (T) statistics: Clustered (CL), random (RN) and Quasi-periodic (QP)

Dahmen, Fisher, Ertas, Ramanathan, Ben-Zion (PRL, 97; PRE, 98)

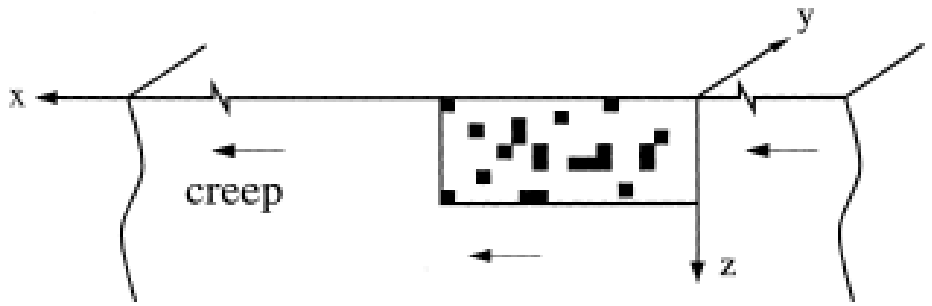

$$\epsilon = (\tau_s - \tau_d)/\tau_s = \text{dynamic weakening}$$

No dynamic-weakening $\tau_s = \tau_d$

Full dynamic-weakening $\tau_d = 0$

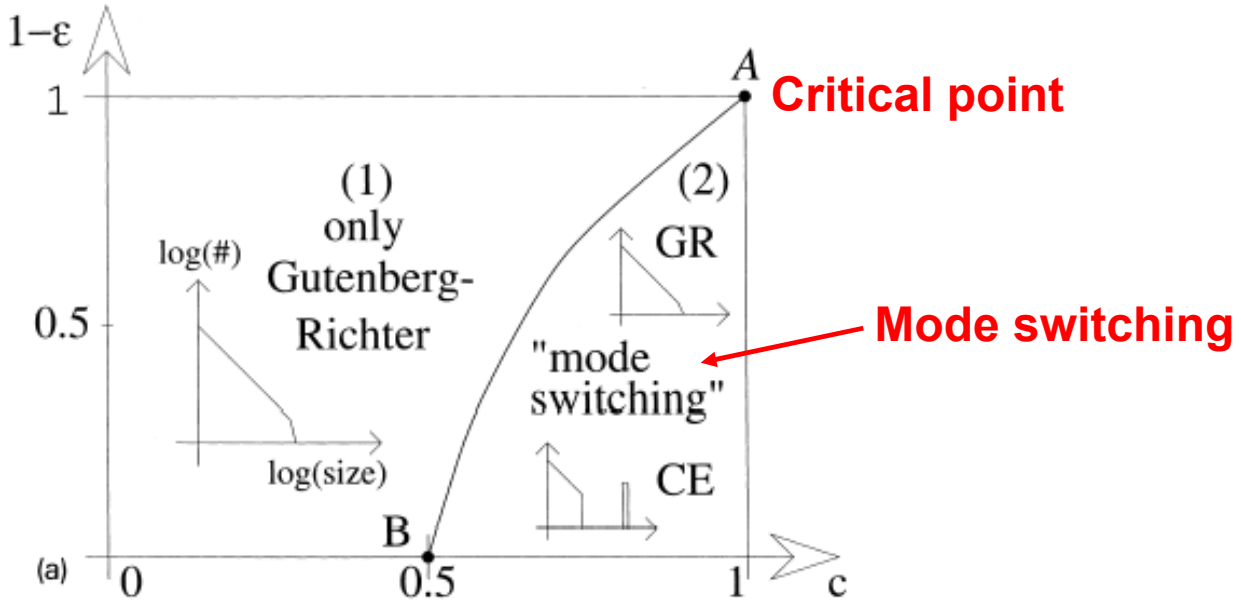

Critical point

Mode switching

Conservation of elastic stress transfer

Criticality

Slip on a fault during a single earthquake

$M_0 \propto S$

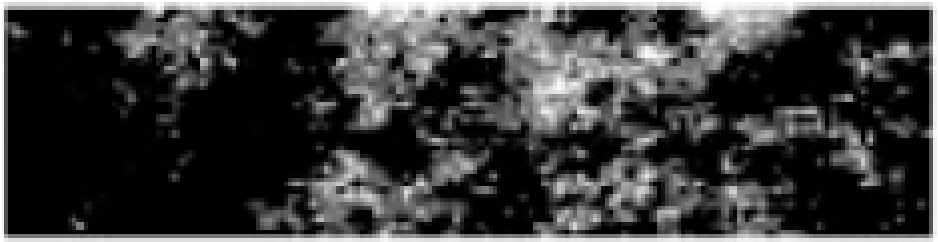

Fractal slip distribution for model at criticality

$\epsilon = 0$

$M_0 = c\Delta\sigma_{static} S^{3/2}$

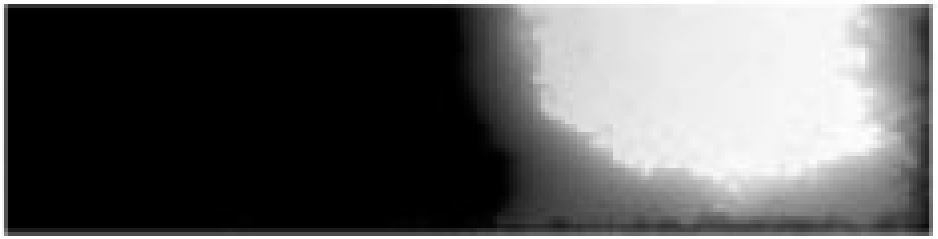

Crack-like slip away from the critical point

$\epsilon > 0$

Average stress on a fault

$\epsilon > 0$

$\epsilon = 0$

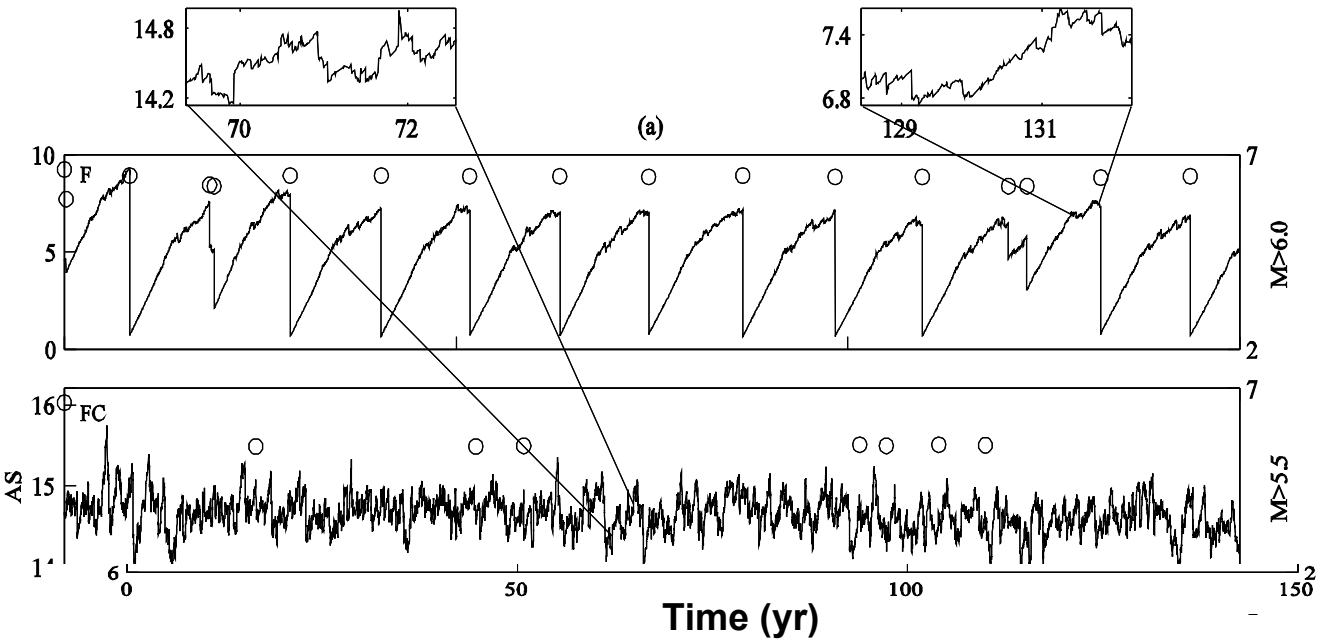

Frequency-size distribution

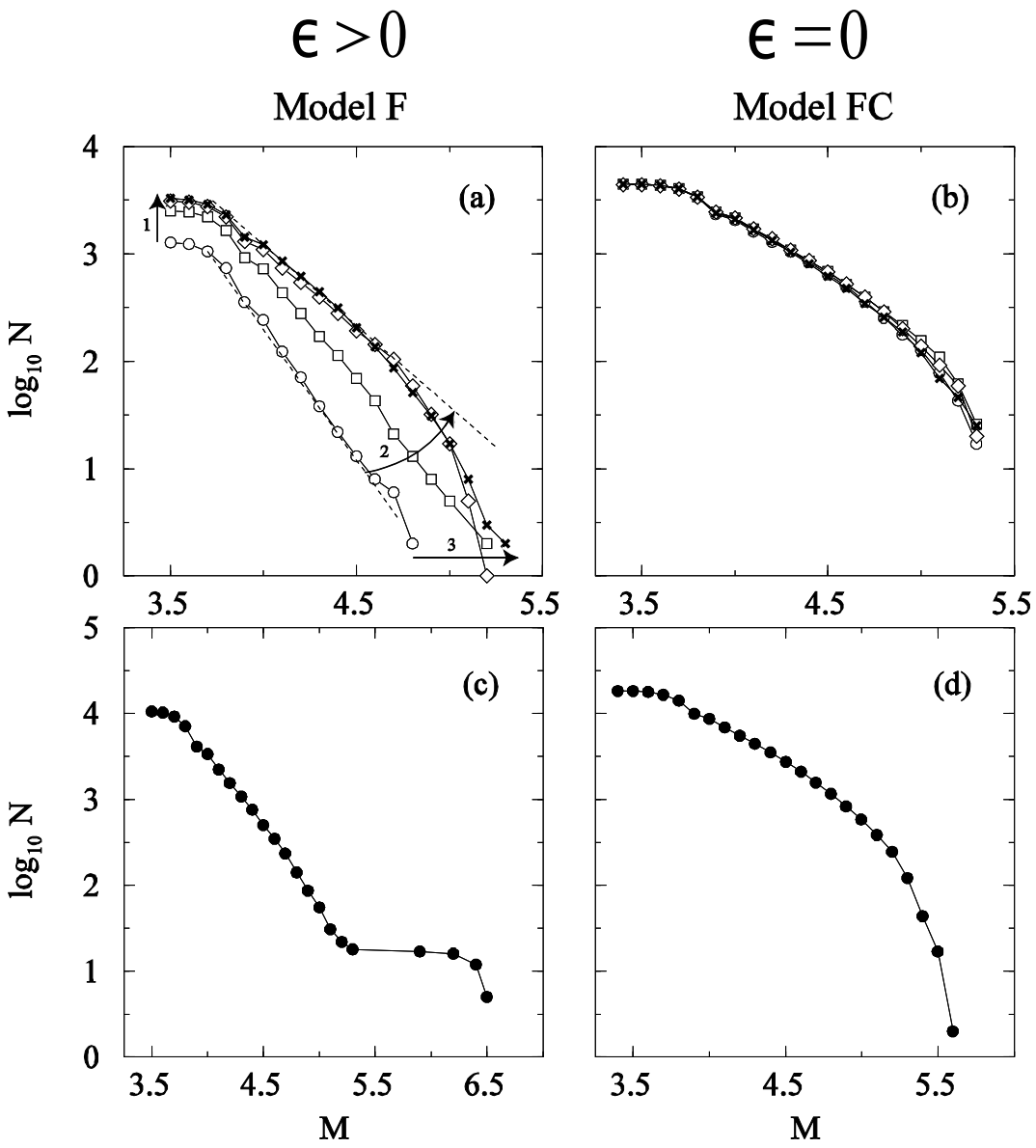

Corresponding differences exist for narrow vs. wide ranges of size scales (Zöller et al.,05)

Mode-switching behavior

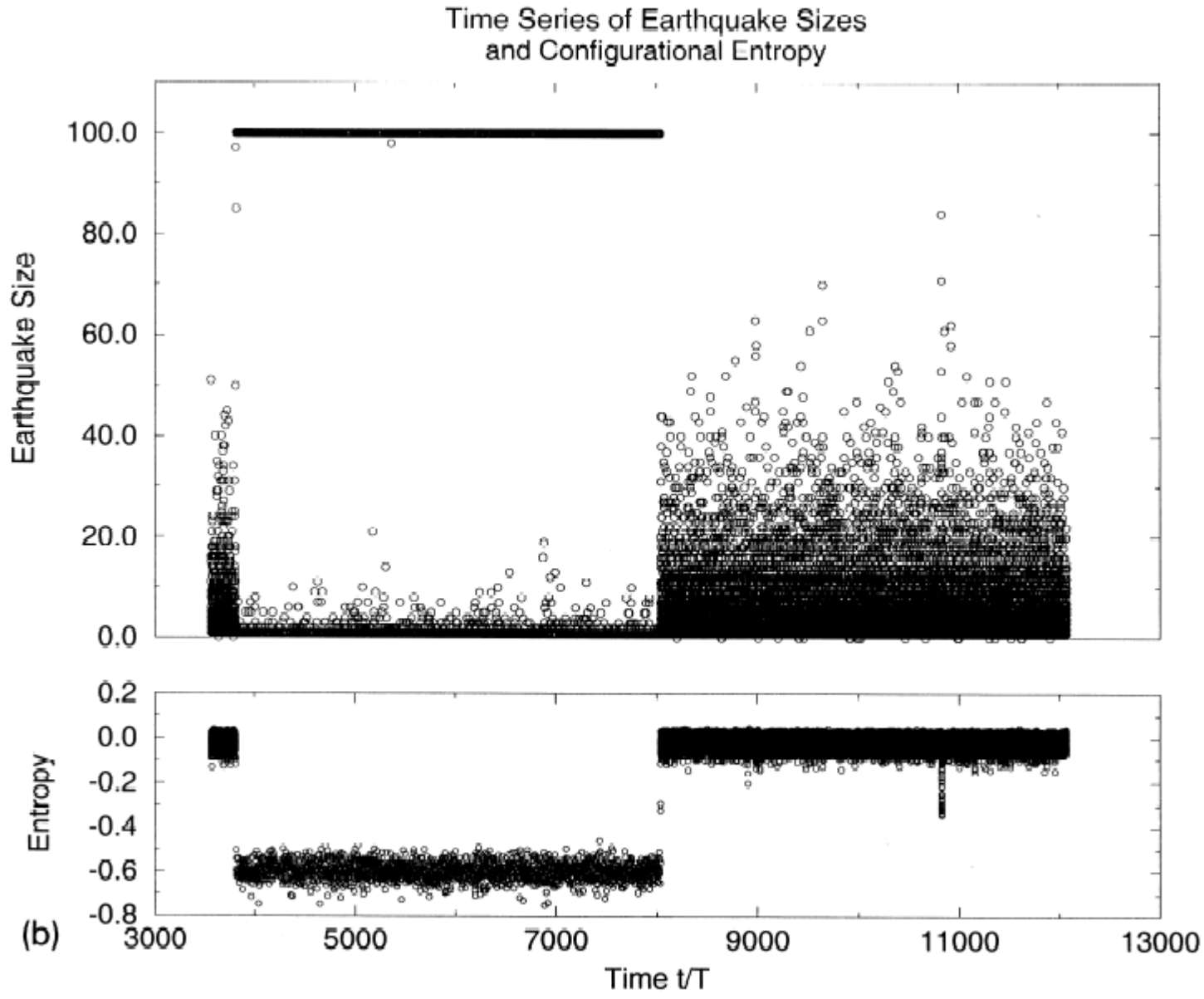

Relations to observations?

Marco et al., JGR, 1996

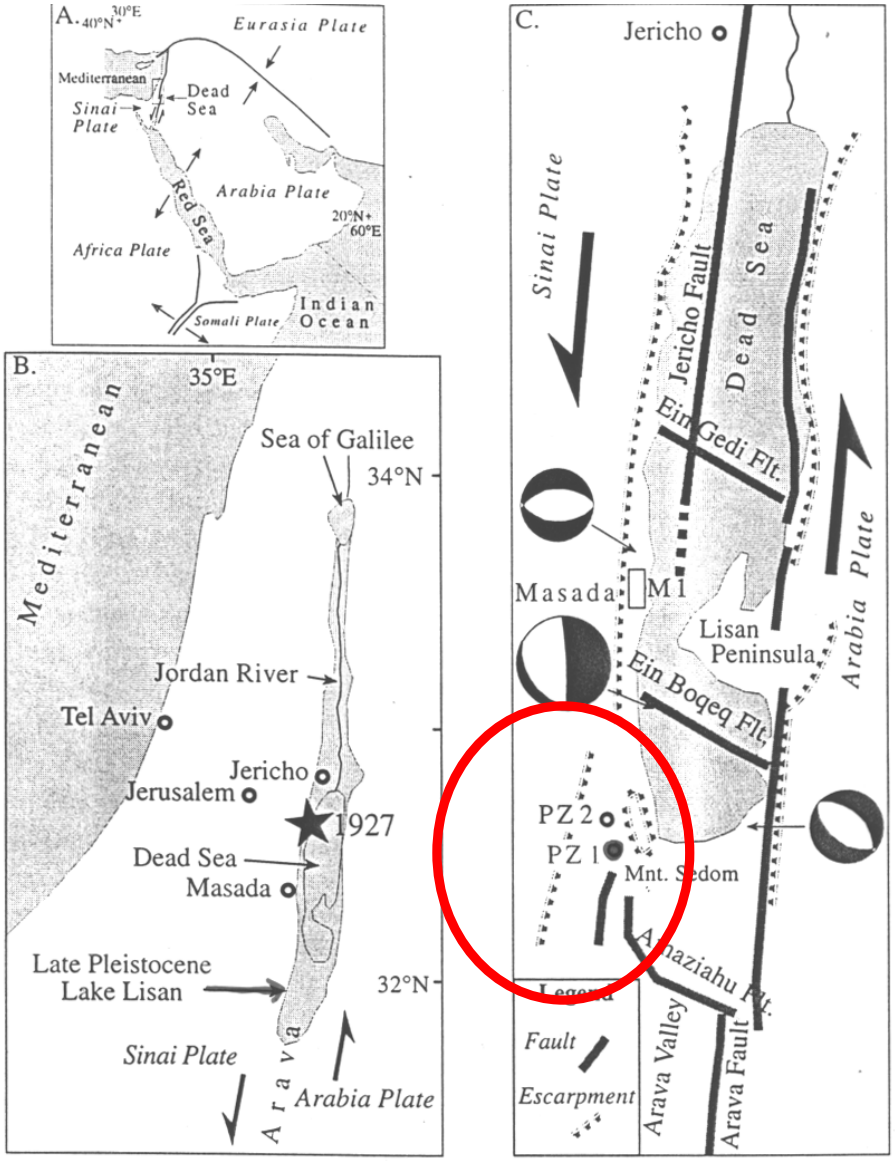

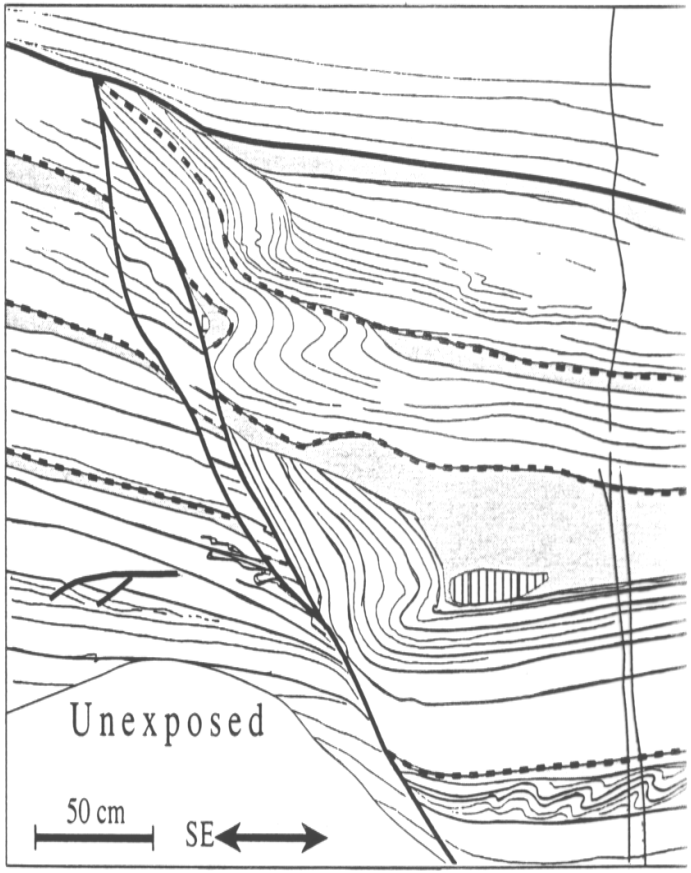

Statistics compatible with mode-switching behavior

JOURNAL OF GEOPHYSICAL RESEARCH, VOL. 101, NO. B3, PAGES 6179–6191, MARCH 10, 1996

Long-term earthquake clustering: A 50,000-year paleoseismic record in the Dead Sea Graben

Shmuel Marco,[1] Mordechai Stein, and Amotz Agnon
Institute of Earth Sciences, Hebrew University, Jerusalem, Israel

Hagai Ron
Institute for Petroleum Research and Geophysics, Holon, Israel

Abstract. The temporal distribution of earthquakes in the Dead Sea Graben is studied through a 50,000-year paleoseismic record recovered in laminated sediments of the Late Pleistocene Lake Lisan (paleo-Dead Sea). The Lisan represents more than 10 times the 4000 years of historical earthquake records. It is the longest and most complete paleoseismic record along the Dead Sea Transform and possibly the longest continuous record on Earth. It includes unique exposures of seismite beds (earthquake-induced structures) associated with slip events on syndepositional faults. The seismites are layers consisting of mixtures of fragmented and pulverized laminae. The places where the seismites abut syndepositional faults are interpreted as evidence for their formation at the sediment-water interface during slip events on these faults. Thicker sediment accumulation above the seismites in the downthrown blocks indicates that a seismite formed at the water-sediment interface on both sides of the fault scarps. Modern analogs and the association with surface ruptures suggest that each seismite formed during a $M_L \geq 5.5$ earthquake. The ^{230}Th-^{234}U ages of a columnar section, obtained by thermal ionization mass spectrometry, give a mean recurrence time of ~1600 years of $M_L \geq 5.5$ earthquakes in the Dead Sea Graben. The earthquakes cluster in ~10,000-year periods separated by quiet periods of similar length. This distribution implies that a long-term behavior of the Dead Sea Transform should be represented by a mean recurrence of at least 20,000 year record. This observation has ramifications for seismic hazard assessment based on shorter records.

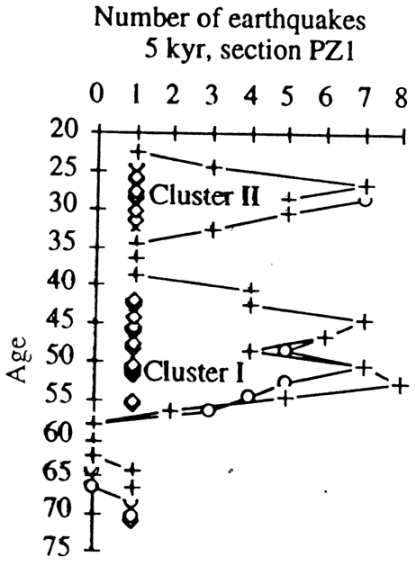

Figure 10. (left) The distribution of mixed layers (i.e., earthquakes) along section PZ1; open diamonds show the individual layers. Crosses and open circles are the number of earthquakes per 5 kyr sliding window, shifted by 2-kyr increments leaving 3-kyr overlap. The crosses show the distribution when the ages of the mixed layers are calculated by a single linear regression, whereas the circles show the distribution when the ages are calculated in three segments (Figure 3). The distribution shows two clusters of frequent events. A cycle about 20,000 years long includes a cluster period and a quiet intercluster period. The pattern of clustering is independent of our choice of calculated sedimentation rates. (right) The distribution of individual mixed layers along sections PZ1, PZ2, and M1. The top of the Lisan is used as a datum. All three sections show clusters of mixed layers separated by quiescent intervals.

Other examples compatible with mode-switching behavior:

50 kyr paleoseismic record along the Arava segment of the DST south of the study area of Marco et al. [Leonard et al., 1998; Amit et al., 2002]

Changes in the character of activity along several faults in the basin and range, western US, province [Wallace, 87],

Episodic clustering of activity in the last 10 kyr years along fault segments in the Eastern CA Shear Zone [Rockwell et al., 2000]

Changes in the character of accumulation and release of seismic energy on the San Miguel fault, Mexico [Hirabayashi et al., 96]

Several widely separated periods with and without large earthquakes in the new Madrid, eastern US, seismic zone [Sexton and Jones, 86]

Episodic clusters of large historic earthquakes in the middle east [Nur, 98] and east Asia [Kyung et al., 96]

(III) Coupled evolution of regional earthquakes and faults in a regional model

[e.g., Lyakhovsky et al., 1997, 2001, 2005; Ben-Zion and Lyakhovsky, 2002, 2006; Hamiel et al., 2004; Finzi et al., 2007].

Thermodynamics-Based Continuum Damage Rheology

- Generalized nonlinear strain energy function extending Hookean elasticity to account for hysteresis in damaged rocks
- Thermodynamics-based Kinetic equation for a damage state variable (α) representing density of microcracks
- Gradual viscous-like failure beyond a first yielding threshold. Macroscopic brittle instability when the energy function losses convexity
- Parameters constrained by lab fracture and friction data

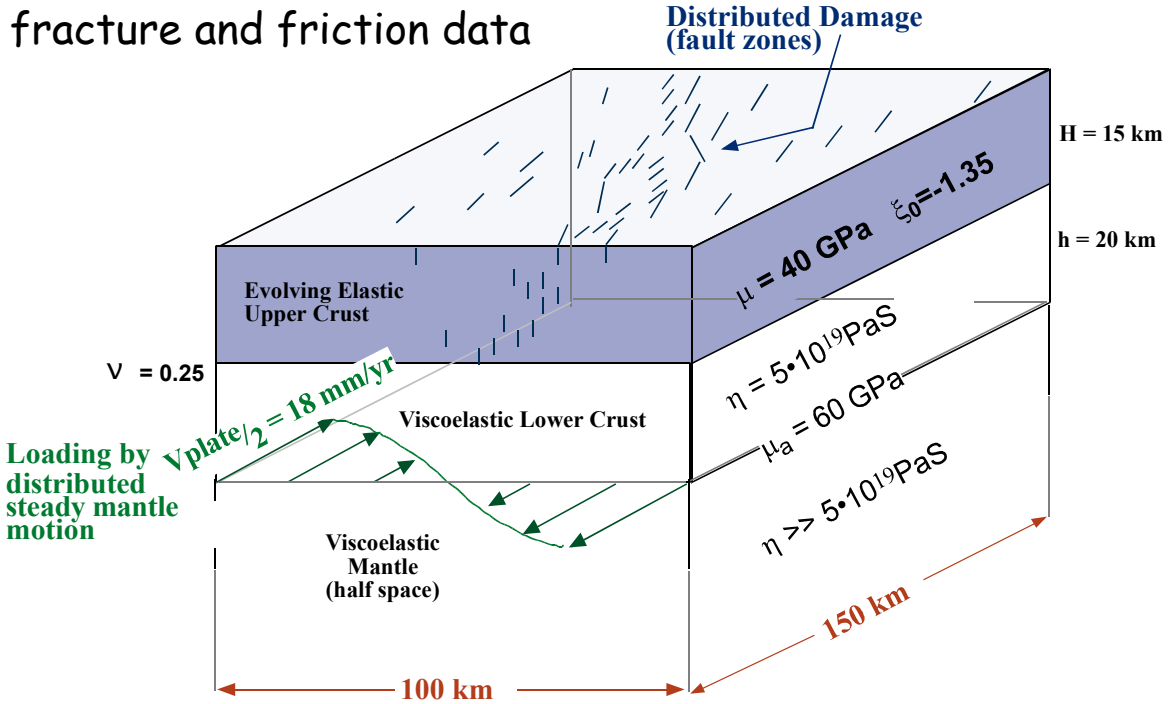

1) Generalized strain energy function of a deforming solid and a third modulus γ for damaged material

:The elastic energy U is written as

$$U=\frac{1}{\rho}\left(\frac{\lambda}{2}I_1^2+mI_2-gI_1\sqrt{I_2}\right) \qquad \xi=\frac{I_1}{\sqrt{I_2}}$$

Where λ and μ ; are Lame constants $\mathbf{I_1=\epsilon_{kk}}$

γ is an additional elastic modulus $\mathbf{I_2=\epsilon_{ij}\epsilon_{ij}}$

$$\sigma_{ij}=\rho\frac{\partial U}{\partial \epsilon_{ij}}=\left(\lambda-\gamma\frac{\sqrt{I_2}}{I_1}\right)I_1\delta_{ij}+\left(2\mu-\gamma\frac{I_1}{\sqrt{I_2}}\right)\epsilon_{ij}$$

2) The elastic moduli are made functions of a damage state variable $\alpha(x, y, z, t)$, representing crack density in a unit volume, and governed by a thermodynamics-based evolution equation

Thermodynamics

Free energy of a solid, F, is

$$F = F(T, \epsilon_{ij}, \alpha)$$

T – temperature, ϵ_{ij} – elastic strain tensor,

α – scalar damage parameter

Energy balance

$$\frac{dU}{dt} = \frac{d}{dt}\left(F + TS\right) = \frac{1}{\rho}\sigma_{ij} e_{ij} - \nabla_i J_i$$

Entropy balance

$$\frac{dS}{dt} = -\nabla_i \left(\frac{J_i}{T}\right) + \Gamma$$

Gibbs equation

$$dF = -SdT + \frac{\partial F}{\partial \epsilon_{ij}} d\epsilon_{ij} + \frac{\partial F}{\partial \alpha} d\alpha$$

The internal entropy production rate per unit mass, Γ, is:

$$\Gamma = -\frac{J_i}{\rho T^2}\nabla_i T + \frac{1}{T}\sigma_{ij} e_{ij} - \frac{1}{T}\frac{\partial F}{\partial \alpha}\frac{d\alpha}{dt} \geq 0$$

3) The damage parameters are constrained by lab fracture and friction data

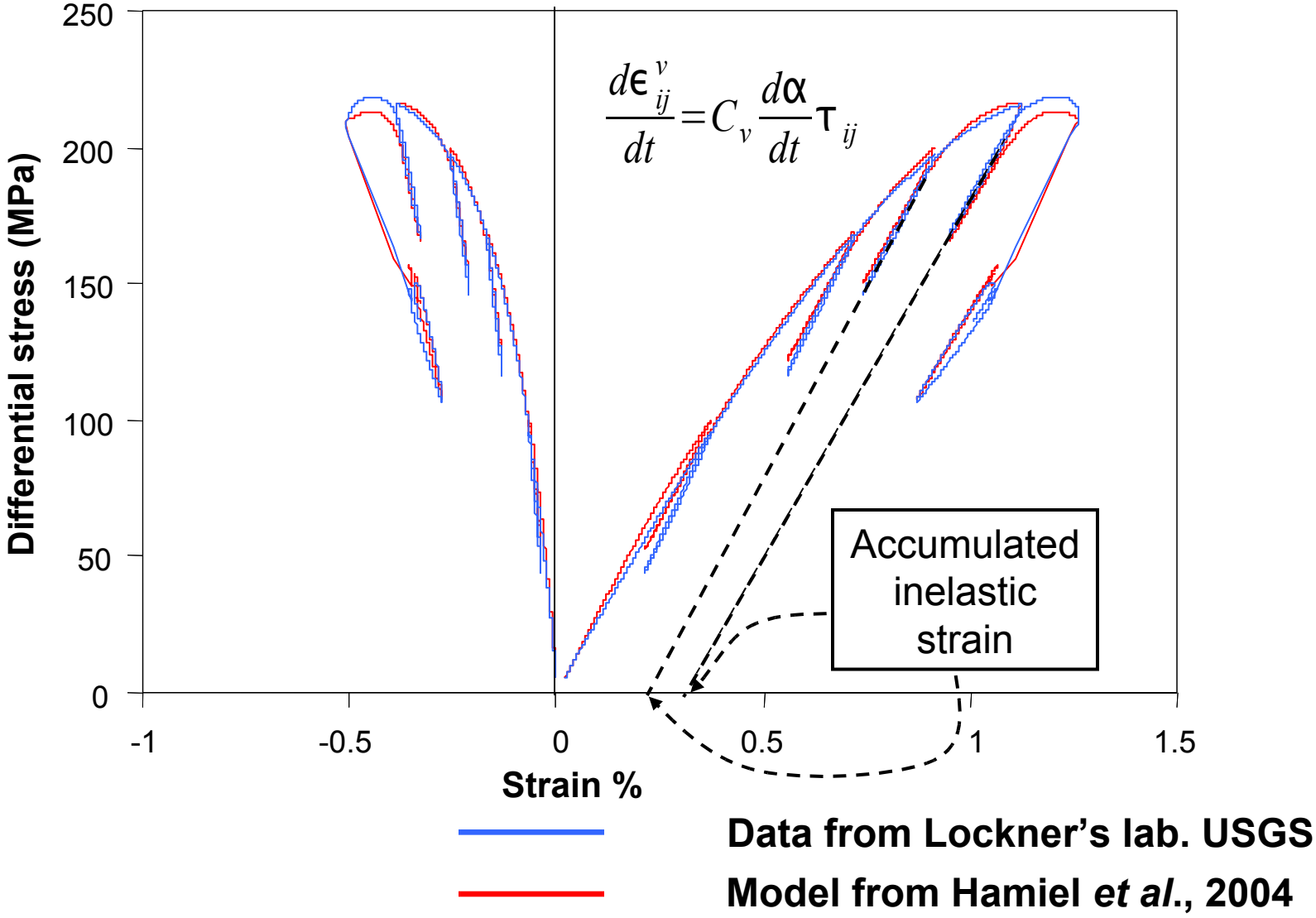

Berea sandstone under 50 MPa confining pressure

Rate- and state-dependent friction experiments constrain parameters c_1 and c_2.

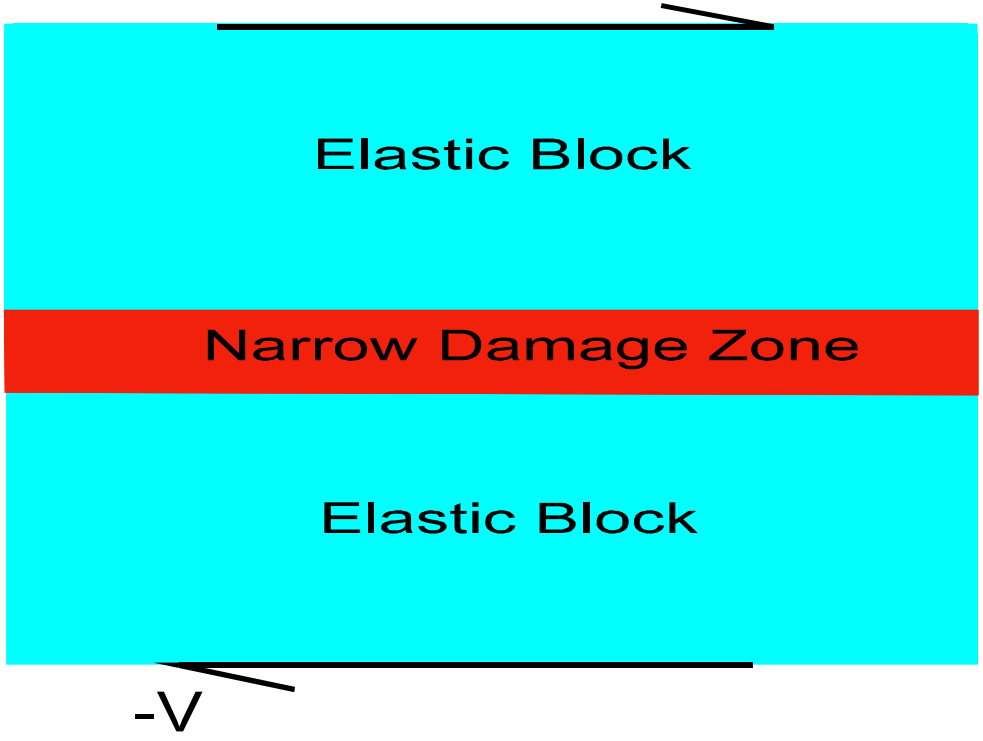

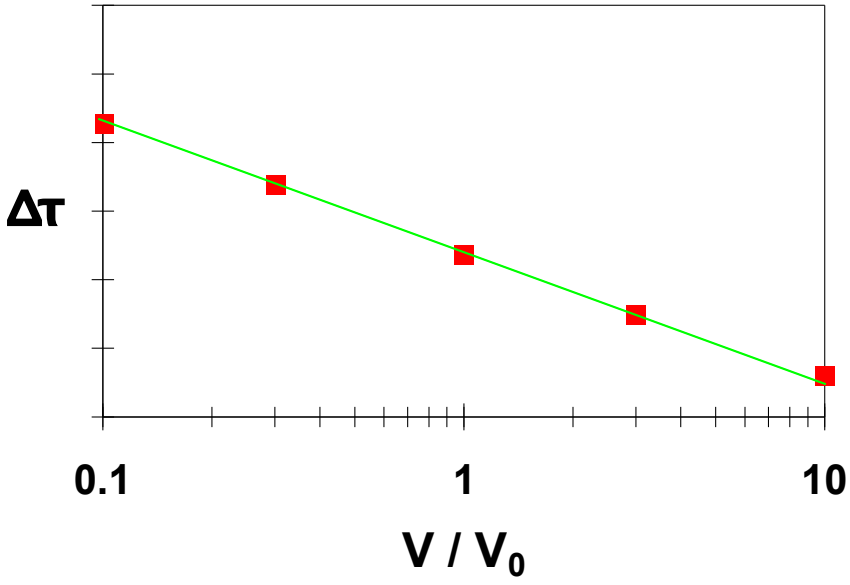

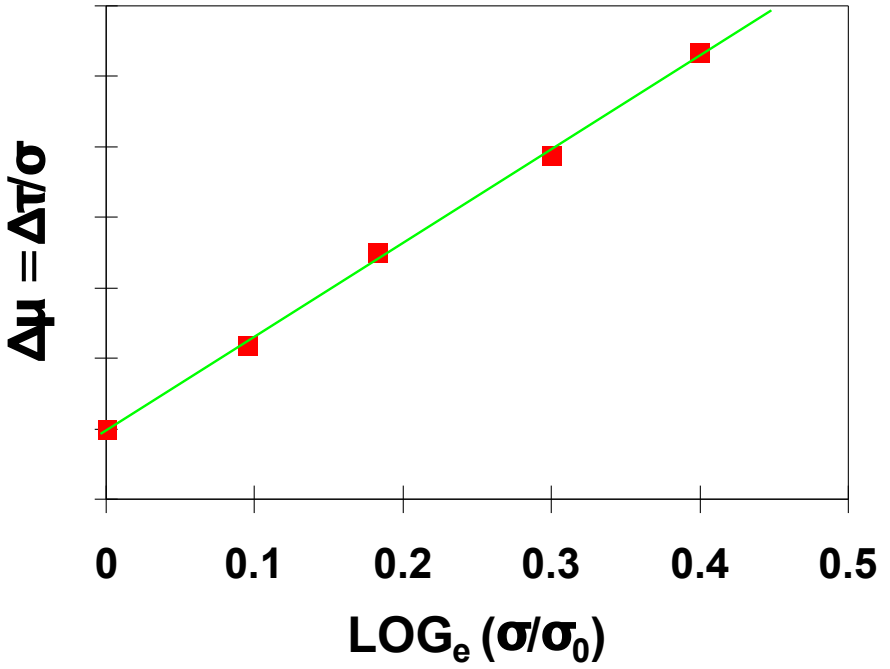

Lyakhovsky *et al.*
(GJI, 2005)

3-D internal structure of a newly created strike-slip fault

Lyakhovsky and Ben-Zion (2007)

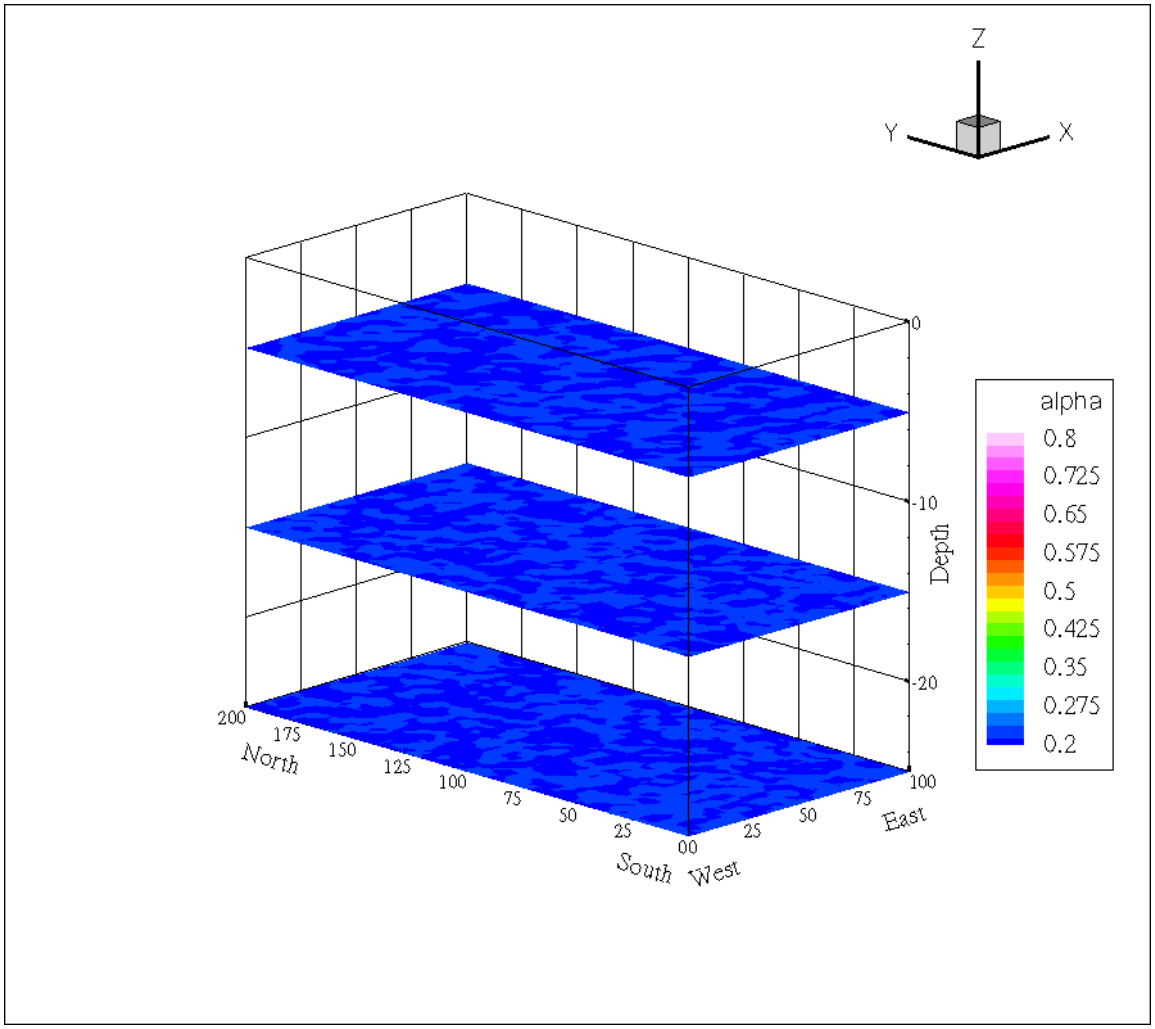

Evolving damage at 5, 15 and 25 km depth. R = 0.5

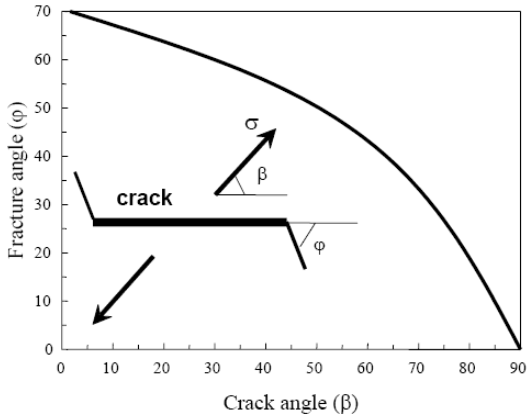

Erdogan & Sih (1963)

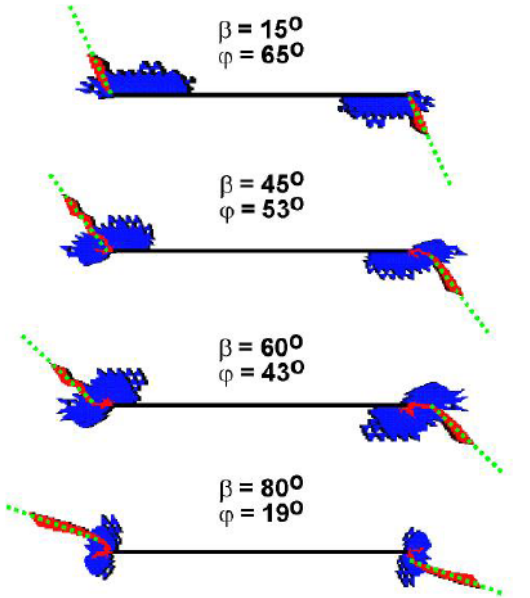

Lyakhovsky and Ben-Zion (2007)

Coupled evolution of earthquakes and faults in a regional lithospheric model

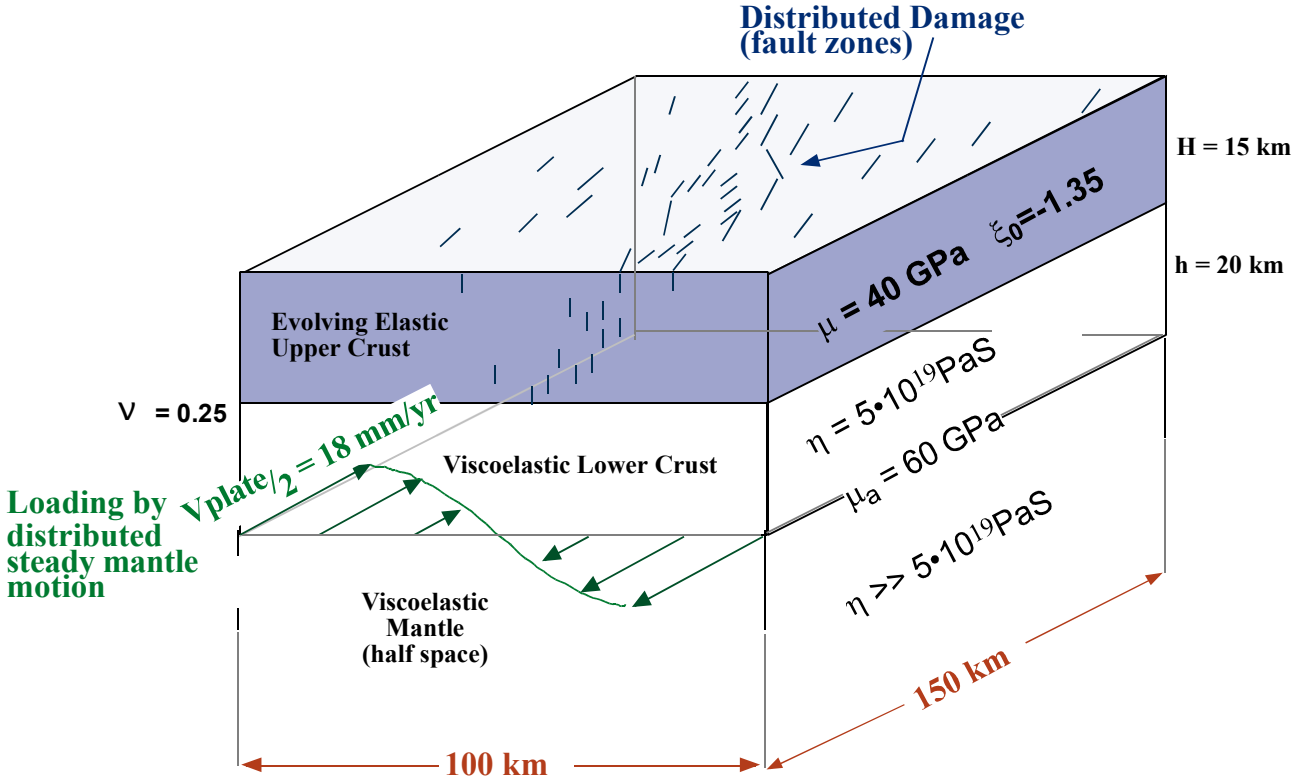

We fix all the large scale parameters (e.g., dimensions, background elastic properties, viscosity) **using data associated with the San Andreas fault.**

The evolving results depend on the ratio of time scale for damage healing τ_H to time scale for tectonic loading τ_L

slow effective healing

Random initial damage distribution

fast effective healing

Weak upper crust,
low friction angle

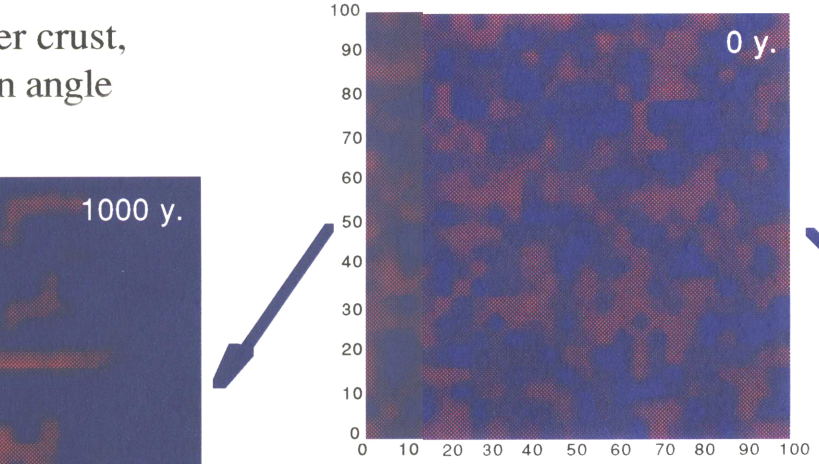

Strong upper crust,
high friction angle

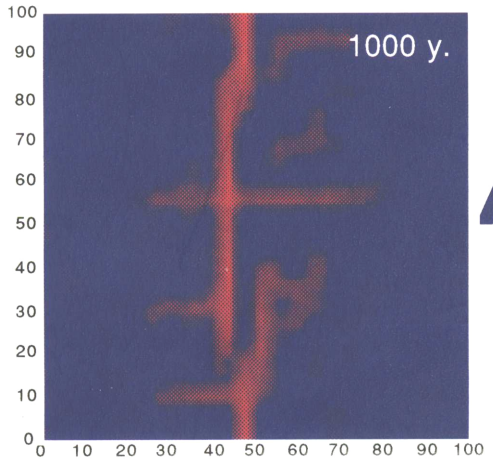

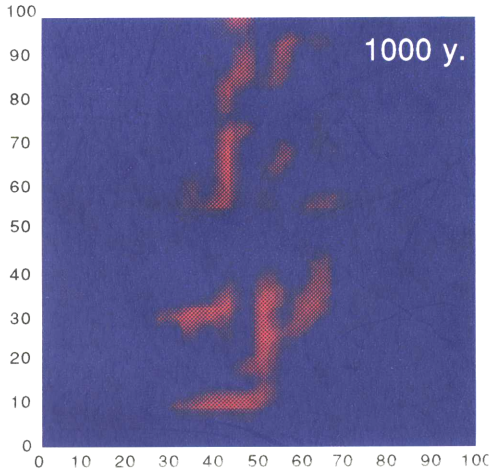

Damage self organization

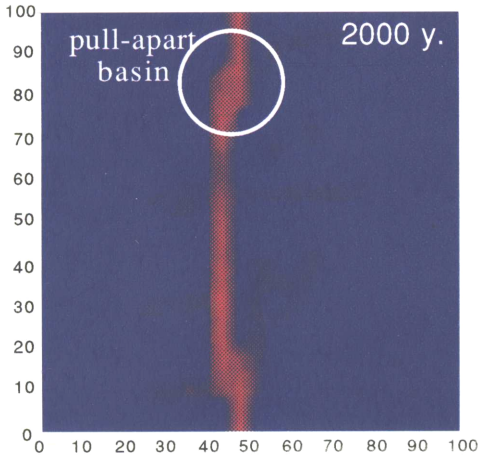

Note the different geometry and rate of damage zone formation between the strong (right) and weak (left) upper crust

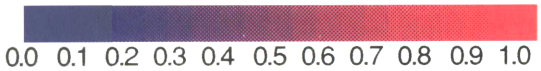

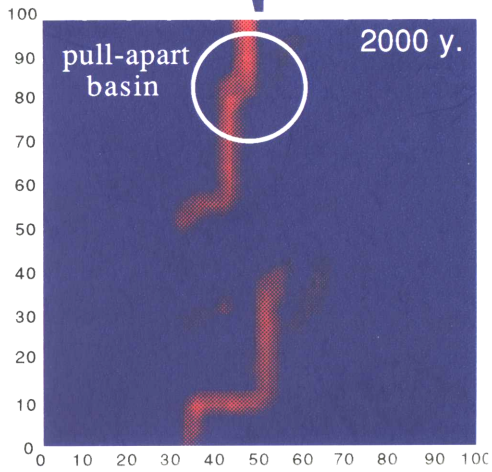

Mode-switching behavior

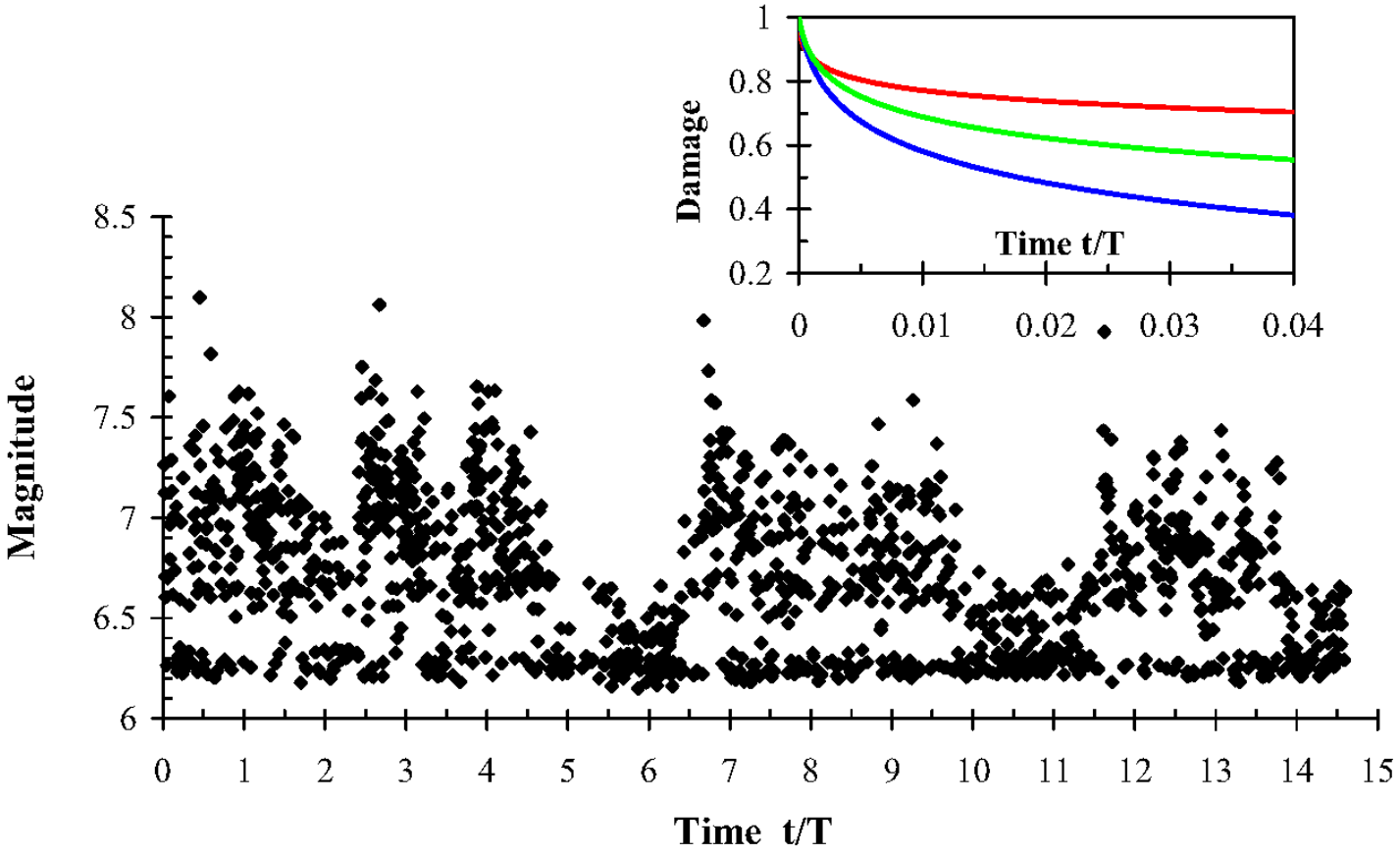

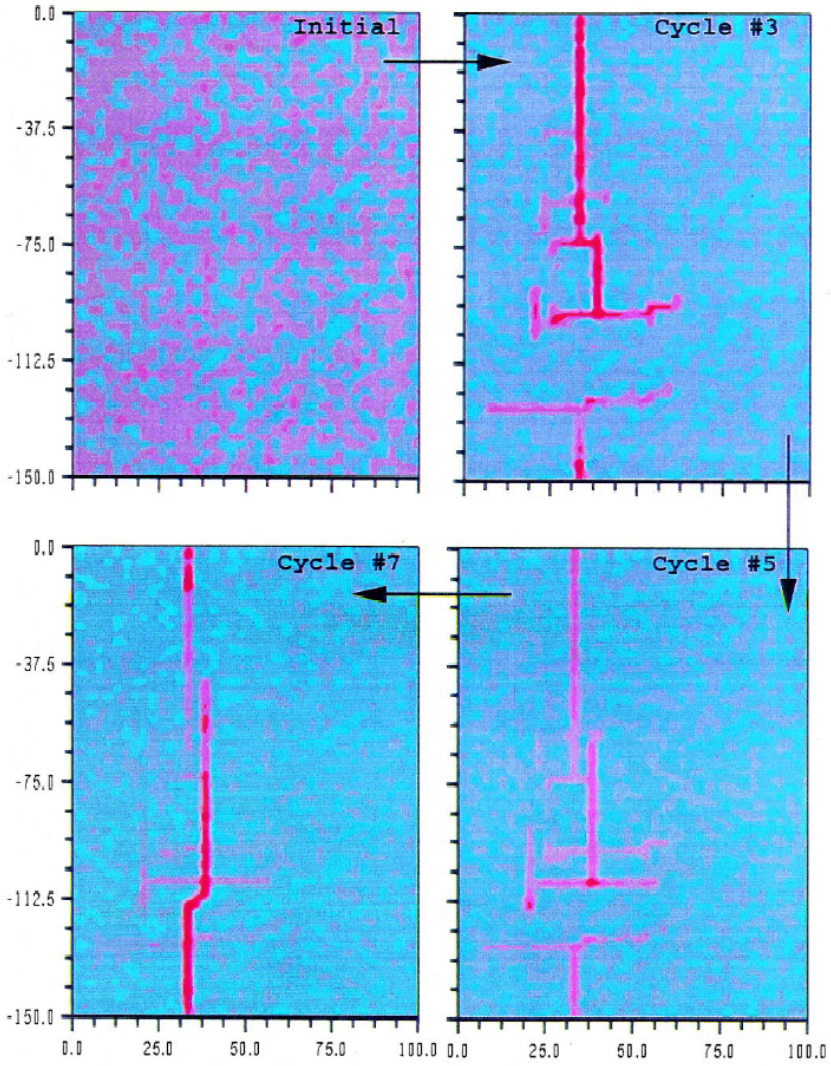
Initial
Cycle #3
Cycle #5
Cycle #7
0.0
-37.5
-75.0
-112.5
-150.0
0.0
25.0
50.0
75.0
100.0
Damage (α)
0
0.5
1

Accelerated Seismic Release

Large earthquakes are sometimes preceded by phases of accelerated seismic release (ASR) in a broad region around the eventual rupture zone

ASR phases were characterized by cumulative Benioff strain following a power law time-to-failure relation with a term $(t_f - t)^m$ with observed values of m are close to 0.3.

$$\sum M_0^{1/2} = A + B\left(t_f - t\right)^m$$

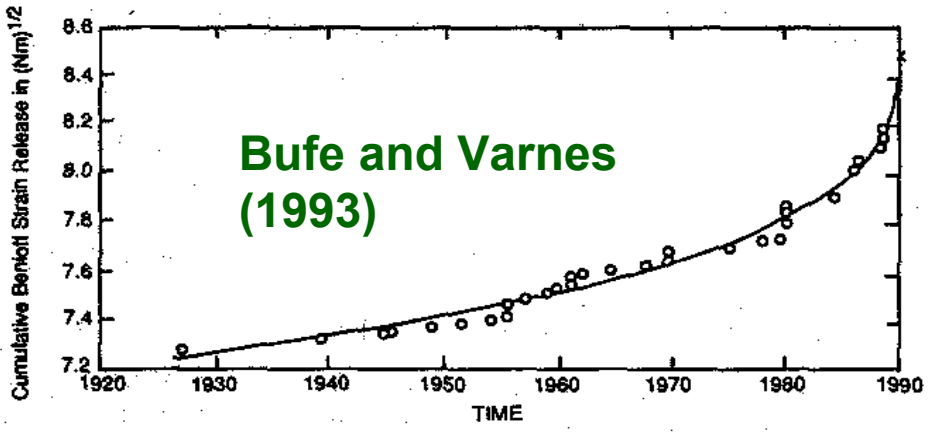

Jaume' and Sykes (1990)

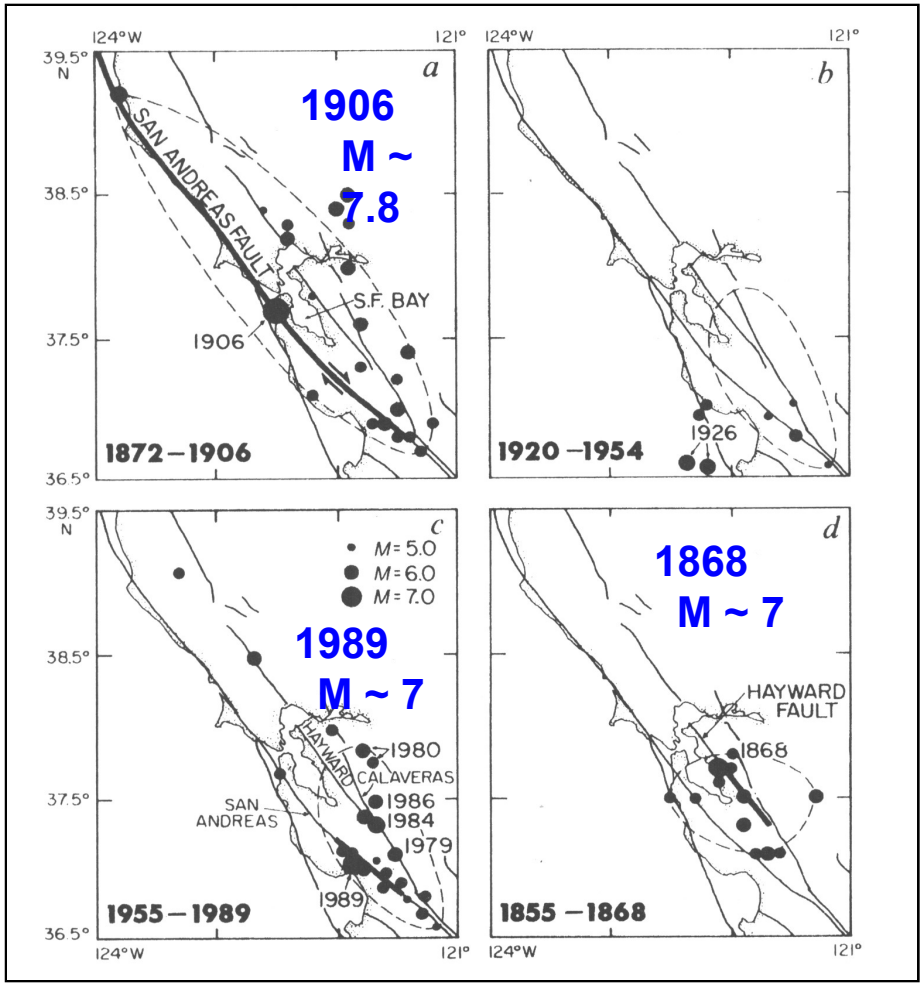

A 1D version of the damage model leads analytically to time-to-failure relation for strain with m=-1/3 and cumulative Benioff strain release with m=1/3.

For 1D deformation, the equation for damage evolution becomes

$$d\alpha/dt = C\,\epsilon^2, \qquad (1)$$

where ϵ is the current strain.

The stress-strain relation in this case is

$$\sigma = E_0(1 - \alpha)\epsilon\ , \qquad (2)$$

where $E_0(1 - \alpha)$ is the effective elastic modulus of a 1D damaged material with E_0 being the initial modulus of the undamaged solid.

Assuming constant stress σ and integrating (1) using (2) gives

$$\alpha = 1 - \{1 - (3C\sigma^2/E_0^{\,2})t\}^{1/3}. \qquad (3)$$

Substituting (3) back into (2) leads to strain accumulation in the power law form

$$\epsilon = \sigma/E_0\{1 - (3C\sigma^2/E_0^{\,2})t\}^{-1/3}. \qquad (4)$$

Using in (4) $t_f = E_0^{\,2} / 3C\sigma^2$, defined by setting $\alpha = 1$ in (3), and changing constants gives

$$\epsilon(t) = \sigma/E_0\,(1 - t/t_f)^{-1/3} = \sigma/E_0\,(\Delta t/t_f)^{-1/3} \qquad (5)$$

with $\Delta t = t_f - t$.

Equation (5) with negative exponent and strain singularity at the final failure provides appropriate physical expression for evolving deformation preceding system-size event. However, analysis of observed ASR phases to date focused on a non-singular power law time-to-failure equation of cumulative Benioff strain release with a positive exponent.

Such an expression can be derived from the previous results as follows.

Using (2)-(5), the strain energy is

$$U(t) = (1/2)\sigma\epsilon = (\sigma^2/2E_0)(\Delta t/t_f)^{-1/3}, \quad (6)$$

the energy and moment releases are proportional to

$$-\partial U/\partial t \sim -(\Delta t/t_f)^{-4/3}, \quad (7)$$

and the cumulative Benioff strain release is proportional to

$$-\int(\partial U/\partial t)^{1/2}\, dt \sim (\Delta t/t_f)^{1/3}. \quad (8)$$

Thus the 1D version of the damage rheology predicts a power law time-to-failure relation for cumulative Benioff strain with an exponent $m = 1/3$.

A related expression with a constant background strain is

$$\sum M_0^{1/2}(t) = A_1 + A_2 t + A_3(\Delta t/t_f)^{1/3} \quad (9)$$

where A_1, A_2, A_3 are constants

3-D simulations results

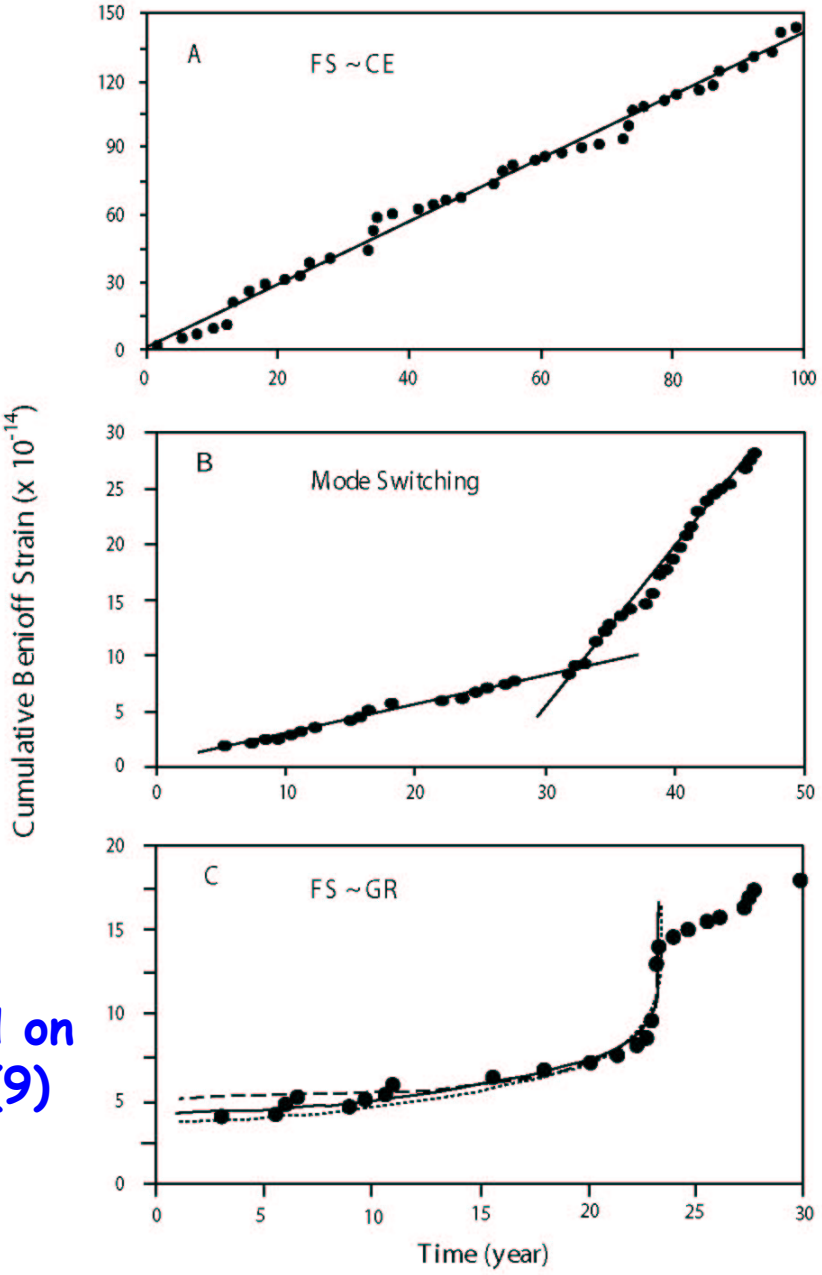

The line fits are based on equations (5), (8) and (9)

Evolution of seismicity in accelerated release phase

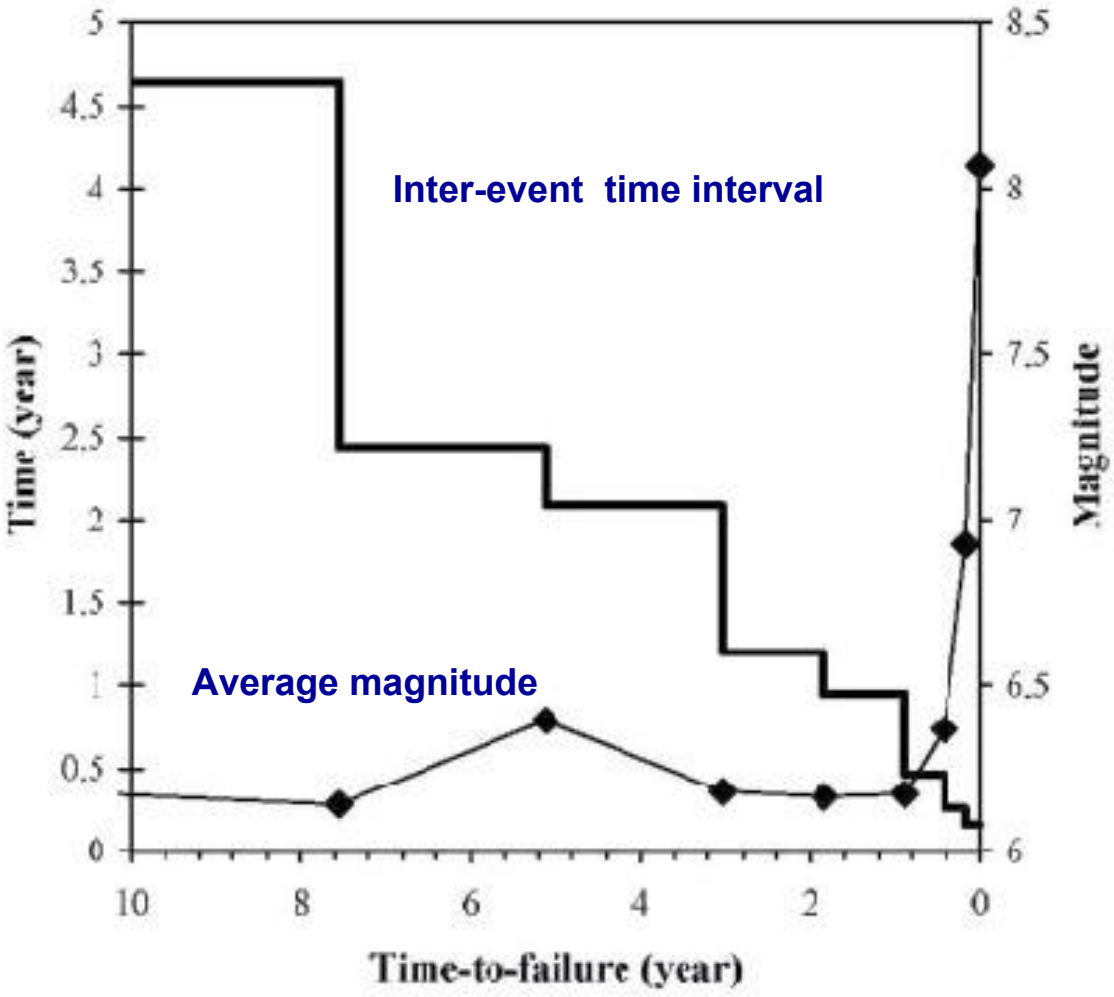

Main Results

There are 3 general dynamic regimes:

- The first is associated with relatively smooth faults, FS statistics compatible with the characteristic earthquake distribution, quasi-periodic temporal occurrence of large events, and no accelerated seismic release.

- The second is associated with disordered fault structures, power law FS statistics of earthquakes, temporal clustering of intermediate and large events, and accelerated seismic release before large earthquakes.

- For a range of conditions, there is a third regime in which the response switches back and forth between the forgoing two modes of behavior over multiple large earthquake cycles.

- In the latter cases, the seismic response of the fault zone is non-stationary on time scales shorter than several mode-switching intervals (e.g., 1000-10000 yr. for large fault zones).

- Cold regions have classical aftershock sequences with power law frequency-size statistics, while warm/hot regions have diffuse sequences or swarms without power law frequency-size statistics.

Thank you